

**Electric spark energy required for igniting  
transient clouds of lycopodium dust in air using inherent  
dust cloud triggering of spark discharge.  
Influences of selected experimental parameters**

by

Michelle Magtuto



A thesis submitted for the partial fulfilment of  
the requirements to obtain the degree of  
Master of Science in the subject of  
Process Safety Technology

Department of Physics and Technology  
University of Bergen  
Bergen, Norway  
December 2016

## Acknowledgement

I would like to express my deepest gratitude to Professor Bjørn Johan Arntzen, for his supervision, for his unmeasurable patience and encouragement since the start of my admission at the UiB until the end of the course and for honing me which truly brought me this far.

My deepest gratitude to Professor Rolf Kristian Eckhoff who's been an inspiration, throughout my journey in Process Safety, to his wonderful sharing of knowledge towards his passion on different aspects of preventing and mitigating explosion hazards in industries, his words of wisdom, for his supervision and for all his unmeasurable help.

My deepest gratitude to Engineer Werner Olsen for his teaching and supervision on practical field of electrical and electronics, all endeavour that I face throughout my experiment and my safety. He is also an inspiration that I appreciate more the beauty of electrical and electronics.

To my professors, Professor Pawel Jan Kosinski, Professor Bjørn Kvamme and Professor Bjørn Tore Hjertaker, thank you very much.

Also, special thanks to the IFT mechanical workshop personnel who has been so helpful for iteration and for the improvement of my apparatuses. A warm thank you to Irene Heggstad of Electron Microscopy laboratory for assisting me and for a wonderful photograph of *lycopodium clavatum*.

Finally, to my parents Samuel Magtuto Sr. and Melba Magtuto, to my siblings Auruel, Samuel Jr. and Irael and specially to my children Jonelle Astee and John Mitchel Magtuto Dagpin who are truly an inspiration and waiting patiently across the ocean and for the unconditional love and support throughout my studies in Bergen, Norway.

To the University of Bergen, I am forever grateful.

## Abstract

The catastrophic outcome of accidental explosions to humans and property has caused an increased need for new knowledge in order to prevent and mitigate the effects of such events. Amongst other substances, a wide range of gases and dusts can cause such explosions. The present experimental study is concerned with electrostatic-spark-initiation of dust explosions.

*Lycopodium clavatum* was chosen as the test dust, partly because this dust has been widely used in previously published investigations on various aspects of dust explosions. Also, the dust can be obtained throughout the world and research results from various researchers can be compared.

In the present study transient experimental clouds of *lycopodium clavatum* in air were produced by dispersing a given amount of the dust, placed in a small cavity at the bottom of the explosion vessel, by a blast of air. In almost all experiments the nominal dust concentration was stoichiometric. In a few experiments it was twice the stoichiometric. Synchronization of the transient experimental dust cloud and the spark discharge was brought about by the dust cloud itself, when it entered the spark gap that had already been charged to a voltage somewhat below the natural breakdown voltage in just air. This breakdown mechanism may well be one of the mechanisms of dust cloud/spark synchronization that can actually operate in accidental industrial dust explosions initiated by electrostatic spark discharges.

One specific problem studied in the present investigation was the influence of the spark discharge duration on the ease by which the dust cloud could be ignited when using the inherent spark discharge triggering method. It was known from the literature that the lowest electric spark energy that can ignite a dust cloud depends strongly on the discharge time of the spark discharge. In the present experiment the discharge duration was varied by varying the series inductance in the discharge circuit.

The experimental probabilities of ignition, based on 40-100 apparently identical successive experiments, were presented as functions of the spark discharge duration, electrode shape, spark energy and spark resistance. The influence of air humidity on the natural breakdown voltages of the two different spark gap geometries used was also investigated.

The experiments confirmed that the minimum stored capacitor energies required for igniting the dust clouds decreased markedly with increasing spark discharge duration. There was only a modest influence of the spark electrode geometry on the minimum ignition energy (MIE). Experimental correlations between various other parameters were also obtained.

The results obtained have thrown light on the influences of some relevant physical parameters on the likelihood of accidental electrostatic spark ignition of dust clouds. However, there is a clear need for more research in this area, and some suggestions for future studies are indicated.

## Table of contents

<b>Acknowledgement</b> .....	<b>i</b>
<b>Abstract</b> .....	<b>ii</b>
<b>1 Introduction</b> .....	<b>1</b>
1.1 Overall context of present investigation .....	1
1.2 What is dust explosion? .....	1
1.2.1 Historical perspective.....	1
1.2.2 Combustible and non-combustible dust.....	3
1.2.3 Factors influencing the ignitability and explosibility of dust clouds .....	4
1.2.4 Explosive concentration ranges of dust clouds in air.....	5
1.2.5 Primary and secondary dust explosions .....	6
1.2.6 Ignition sources that can ignite dust clouds .....	7
1.2.7 Means of preventing and mitigating dust explosions in the process industries .....	8
1.3 Case history of catastrophic industrial dust explosion in China in 2014.....	10
1.3.1 Overview .....	10
1.3.2 The plant that was struck by the explosion.....	10
1.3.3 Process equipment layout .....	11
1.3.4 Dust collection system and processing equipment .....	11
1.3.5 Explosion development.....	12
1.3.6 Probable ignition source of the initial primary explosion.....	12
1.4 Specific research topic of present thesis .....	13
1.4.1 Introduction.....	13
1.4.2 Electric/electrostatic spark discharges .....	13
<b>2 Review of literature related to the specific topic of the present thesis</b> .....	<b>15</b>
2.1 Experimental studies of electric spark gap breakdown by dust particles .....	15
2.1.1 Investigation by Eckhoff (1970) .....	15
2.2 Influence of spark discharge time on MIE of dust clouds .....	18
2.3 Theory on electrical circuits .....	22
2.4 Breakdown voltage mechanism in the air between two conducting electrodes .....	25
2.5 Breakdown voltage mechanism by dust particles between electrode gap .....	26
<b>3 Experimental apparatus and methods</b> .....	<b>26</b>
3.1 Experimental apparatus .....	26
3.1.1 Explosion vessel.....	27
3.1.2 Electric spark discharge system .....	28

3.1.3	Dust dispersion system .....	29
3.1.4	Measuring instruments .....	30
3.2	Methods .....	31
3.2.1	Electric spark discharge generation .....	31
3.2.2	Dust dispersion system .....	32
3.2.3	Determination of MIE.....	32
3.2.4	Measurement of discharge duration of spark discharges.....	33
3.2.5	Estimation of spark energy .....	34
3.2.6	Estimation of time constant, resistance and current of spark discharge ..	34
<b>4</b>	<b>Test dust .....</b>	<b>37</b>
<b>5</b>	<b>Results .....</b>	<b>38</b>
5.1	Electric spark discharge decaying oscillation including the duration .....	38
5.1.1	Mass of dispersed dust .....	42
5.1.2	Dispersion air pressure.....	43
5.2	Estimated theoretical spark energies by two different methods .....	44
5.3	Estimated time constants, resistances and currents of spark discharge .....	46
5.4	MIE of lycopodium clavatum at nominal stoichiometric dust concentration.	48
5.5	Parameters that affects the ignition of lycopodium dust cloud .....	50
5.5.1	Dispersion air pressure.....	50
5.5.2	Concentration of lycopodium dust.....	51
5.6	The relationship of spark resistance and energy.....	51
5.7	Actual breakdown voltage in air and the set supply voltage difference .....	53
5.8	Simulation of spark current and voltage as a function of time .....	53
5.9	Additional phenomenon observed. ....	54
<b>6</b>	<b>Discussion.....</b>	<b>56</b>
6.1	Practical industrial scenario for which the present investigation is relevant..	56
6.2	Electric spark discharge decaying oscillation including the duration .....	57
6.3	Spark energies.....	57
6.4	Time constant, resistance and current.....	58
6.5	Minimum ignition energy .....	58
6.6	Difference between set supply voltage and actual breakdown voltage .....	59
6.7	Delay of electric spark discharge and captured flamelet .....	60
6.8	The influence of electrostatic charge on the wall of the explosion vessel.....	61
<b>7</b>	<b>Conclusions and suggestions for further work.....</b>	<b>61</b>
7.1	Conclusions .....	61

7.2	Suggestion for further work.....	62
<b>References</b>	.....	<b>64</b>
<b>Appendix A</b>	<b>Experimental apparatus and measuring instruments</b> .....	<b>67</b>
<b>Appendix B</b>	<b>Flamelet</b> .....	<b>71</b>

# 1 Introduction

## 1.1 Overall context of present investigation

The overall context of the present thesis is “process safety”. According to Rigas (2012), as discussed by Amyotte (2013), the U.S. Occupational Safety and Health Administration, OSHA (1992) defined the term “process” as “any activity involving hazardous chemicals, including use, storage, manufacturing, handling and on-site movement of such chemicals .....”. The term “process safety” then comprises any effort aimed at preventing and mitigating accidents like explosions, fires, and emission of toxic substances that can cause injury and loss of life, and interruption and damage of processes.

Accidental dust explosion is a potential hazard in many process industries. Dust explosions have caused loss of life, injuries, traumas, environmental problems, and interruption or total loss of business.

## 1.2 What is dust explosion?

Some dusts/powders can give dust explosions, other cannot. As pointed out by Amyotte (2013), difference between dusts that can give dust explosions and those that cannot, were discussed by Morgan and Supine (2008). The term “dust” has been defined by the U.S. National Fire Protection Association (NFPA) as “any finely divided solid having particle diameters less than 420  $\mu\text{m}$  (i.e., material capable of passing through a U.S. no. 40 Standard Sieve)”. According to Amyotte (2013) NFPA (2007) defines a combustible dust as “a combustible particulate solid that presents a fire or deflagration hazard when suspended in air or other oxidizing medium over a range of concentrations, regardless of particle size or shape”.

### 1.2.1 Historical perspective

Accidental dust explosion has been recognized as a real industrial hazard in Europe for at least 2 to 3 centuries. One of the first recorded dust explosion was the wheat flour explosion in a warehouse of Mr. Giacomelli’s bakery in Turin, Italy in 1785. This accident was investigated and reported by Count Morozzo in 1795. When the Academy of Science of Turin heard about Morozzo’s studies, they asked him to prepare a written account of his findings. However, the report of Morozzo did not contain any illustrations. A quite comprehensive summary of the report was given by Eckhoff (2003), accompanied by his own attempt at illustrating a possible scene of the accident, based on the written report of Morozzo. Eckhoff’s illustration is given in Figure 1-1.

The following explanation of what a *dust explosion* is has been taken from chapter 1 in Eckhoff (2003). The basic phenomenon is quite easy to envisage in terms of daily life experience. Any solid material that can burn in air will do so with a violence and speed that increases with increasing degree of sub-division of the material. This is illustrated in Figure 1-2

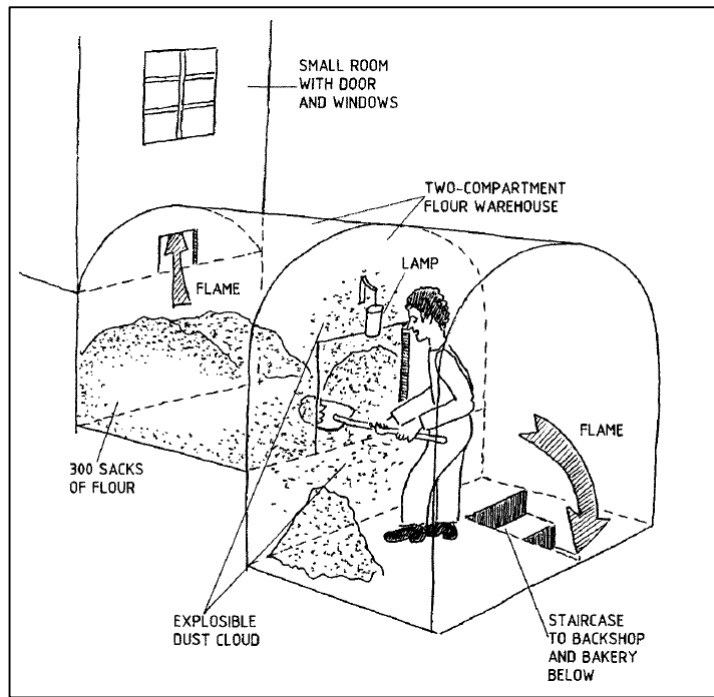


**Figure 1-1: Reconstruction of possible scene of wheat flour explosion in Mr. Giacomelli's bakery on 14th December 1785, as described by Count Morozzo (1795). From Eckhoff (2003).**

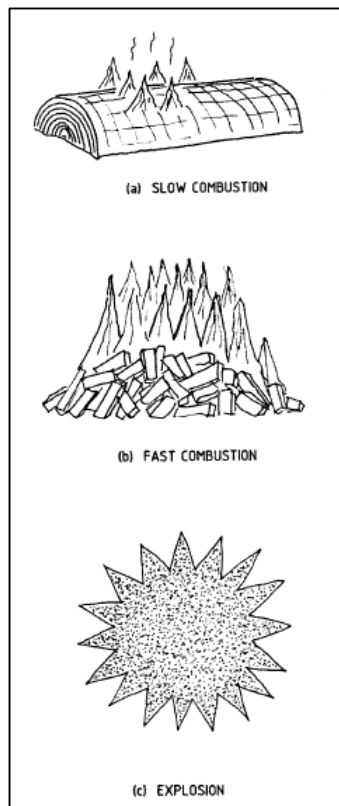


**Figure 1-2: Illustration of the increase of the combustion rate of a given mass of combustible solid increases with sub-division. From Eckhoff (2003).**



Kauffman (1982) was probably the first researcher to introduce the “*dust explosion pentagon*”, as illustrated in Figure 1-3. The pentagon illustrates the five basic conditions that must be satisfied for a dust explosion to occur.

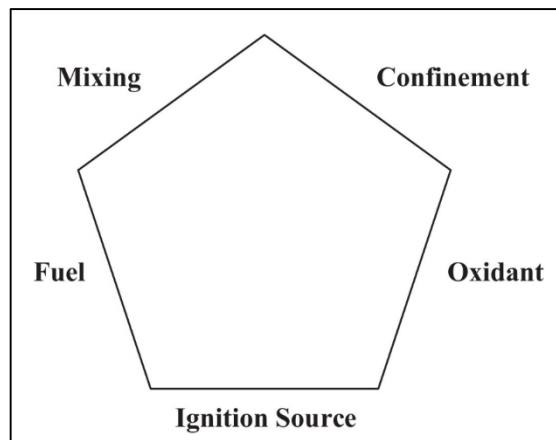
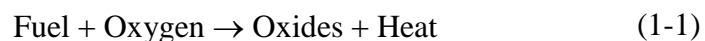


**Figure 1-3: Explosion pentagon. From Kauffman (1982).**

The first condition is that there is a combustible dust or powder (*fuel*). The second and third conditions are that an amount of this dust/powder must somehow be raised into suspension in air (*source of oxygen*) to form a dense, explosible cloud (*dispersion*). The fourth condition is that there must be some *ignition source* that can put the dust cloud on fire. Finally, in order to get the pressure rise that characterizes an explosion, the burning dust cloud has to be *confined* in some way.

### **1.2.2 Combustible and non-combustible dust**

As described by Eckhoff (2003), a dust explosion is caused by rapid release of heat due to the chemical reaction:



Mostly the heat generating process in accidental dust explosions is oxidation by the oxygen in air. However, some metal dusts can react exothermally even with nitrogen or carbon dioxide. The main groups of combustible dusts are:

- Natural organic materials (grain, wood, linen, sugar, etc.).
- Synthetic organic materials (plastics, organic pigments, pesticides, pharmaceuticals, etc.).
- Coal and peat.
- Metals (aluminium, magnesium, titanium, zinc, iron, etc.).

Non-combustible dusts are mostly materials that are already stable oxides:

- Silicates.
- Sulphates.
- Nitrates.
- Carbonates.
- Phosphates

- Portland cement
- Sand.
- Limestone.

The amount of heat that can be liberated in dust explosions varies. To allow a comparison of the violence potentials of explosions presented by various dusts Eckhoff (2003) suggested that the heat of combustion per mole oxygen consumed during combustion would be a useful parameter. This is because the air in given volume of dust cloud contains a given, limited amount of oxygen for combustion, irrespective of the type of dust. In Table 1-1 heats of combustion of various dust materials, per mole of oxygen consumed, is listed together with the conventional heats of combustion.

**Table 1-1: Heats of combustion (oxidation) of various substances per mole O<sub>2</sub> consumed. From Eckhoff (2003).**

Substance	Oxidation product(s)	KJ/mole O <sub>2</sub>
Ca	CaO	1270
Mg	MgO	1240
Al	Al <sub>2</sub> O <sub>3</sub>	1100
Si	SiO <sub>2</sub>	830
Cr	Cr <sub>2</sub> O <sub>3</sub>	750
Zn	ZnO	700
Fe	Fe <sub>2</sub> O <sub>3</sub>	530
Cu	CuO	300
Sucrose	CO <sub>2</sub> and H <sub>2</sub> O	470
Starch	CO <sub>2</sub> and H <sub>2</sub> O	470
Polyethylene	CO <sub>2</sub> and H <sub>2</sub> O	390
Carbon	CO <sub>2</sub>	400
Coal	CO <sub>2</sub> and H <sub>2</sub> O	400
Sulphur	SO <sub>2</sub>	300

### **1.2.3 Factors influencing the ignitability and explosibility of dust clouds**

The basic factors influencing the ignitability and explosibility of dust clouds are:

- Chemical composition of dust, including its moisture content.
- Chemical composition and initial pressure and temperature of gas phase.
- Distribution of particle sizes and shapes in the dust, determining the specific surface area of dust in the fully dispersed state.
- Possibility of significant radiative heat transfer (highly dependent on flame temperature, which in turn depends on particle chemistry).

Factors influenced by the actual industrial dust cloud generation and explosion development:

- Degree of dispersion, or agglomeration, of dust particles in the dust cloud, determining the effective specific surface area available to the combustion process in the dust cloud in the actual industrial situation.
- Distribution of dust concentration in the actual cloud.
- Distribution of initial turbulence in the actual cloud.
- Possibility of generation of explosion induced turbulence in the still unburnt part of the cloud (location of ignition source is an important parameter).
- Possibility of flame front distortion by other mechanisms than turbulence.

All factors stated in this list depend on the nature of industrial process (flow rates, etc.) and the geometry of the system in which the dust cloud burns.

The degree of dispersion or agglomeration of dust particles denotes the formation of dust cloud once suspended in the atmosphere can be perfectly dispersed and poorly dispersed because of agglomeration of dust particles in the cloud will burn as one single large particle This is illustrated in Figure 1-4.

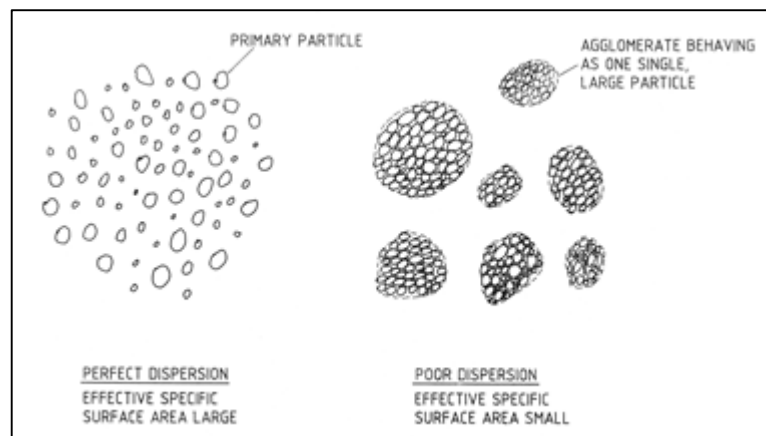


**Figure 1-4: Illustration of perfectly dispersed dust cloud and cloud consisting of agglomerates of much larger effective particle sizes than those of the primary particles. From Eckhoff (2003).**

#### ***1.2.4 Explosive concentration ranges of dust clouds in air***

The *minimum/maximum explosive concentrations* of a dust cloud are the minimum/maximum masses of dust per unit volume of dust clouds that can propagate a self-sustained flame. These explosibility limits are different for various dust materials. High-density materials like metal dusts generally have higher concentration limits than organic dusts. For example, zinc powder has a minimum explosive concentration in air of about 500 g/m<sup>3</sup>.

Figure 1-5 illustrates that typical explosible dust concentration ranges are three to four orders of a magnitude higher than typical hazardous concentration ranges of concern to industrial hygiene. Also, the explosible ranges are narrow, mostly about two orders of magnitude or less. In practice dust clouds of such high concentrations as indicated in Figure 1-5 are mostly found inside the process equipment.

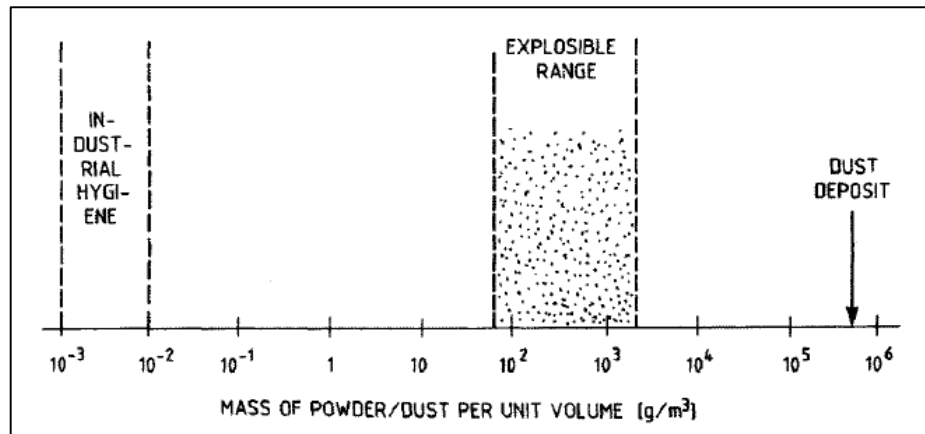


**Figure 1-5: Range of explosive dust concentrations in air at normal temperature and atmospheric pressure of a typical natural organic dust (maize starch), compared with typical range of maximum permissible dust concentrations in the context of industrial hygiene, and a typical density of deposits of natural organic dust. From Eckhoff (2003).**

### 1.2.5 Primary and secondary dust explosions

One prime objective in dust explosion mitigation is to limit the initial/*primary* dust explosion in a process unit to that unit. The big fear is that this explosion may give rise to more serious *secondary* dust explosions outside the process equipment. This is illustrated in Figure 1-6. Therefore, one important aim is to avoid such secondary explosions.

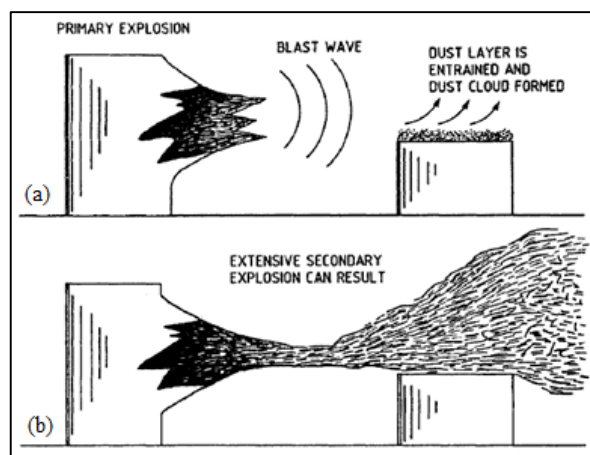


**Figure 1-6: Illustration of how the blast wave from a primary explosion entrains and disperses a dust layer, which subsequently ignites by the primary dust flame. (a) entrains and disperses a dust layer, (b) dust layer is subsequently ignited by the primary dust flame. From Eckhoff (2003).**

There is a gap of about two orders of magnitude between the maximum explosive dust concentration and the bulk density of dust layers and heaps shown in Figure 1-5. The consequence of this with regard to the volume of dust cloud that can be produced by a given volume of dust layer is illustrated in Figure 1-7.

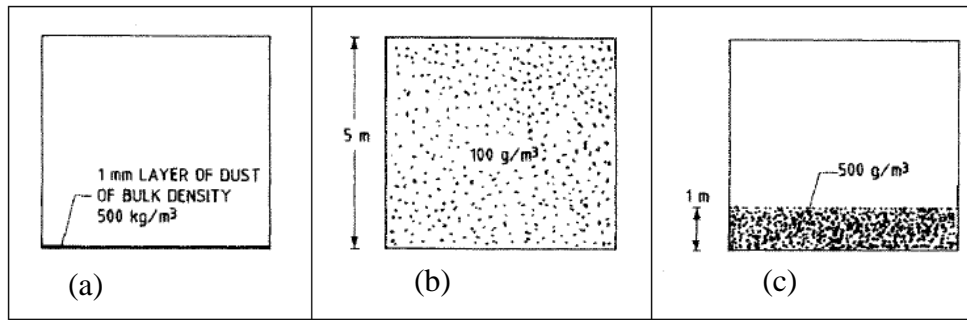


**Figure 1-7: Illustration of the potential hazard of even thin dust layers. (a) 1 mm layer of a dust of bulk density 500 kg/m<sup>3</sup>, (b) generate a cloud of average concentration 100 g/m<sup>3</sup> if dispersed in a room of 5 m height, (c) partial dispersion up to only 1 m gives 500 g/m<sup>3</sup>. From Eckhoff (2003).**

As shown by Eckhoff (2003) the simple calculation behind Figure 1-7 is as follows: If a dust layer of thickness  $h$  and bulk density  $\rho_{bulk}$  on the floor of a room of height  $H$  is dispersed into a homogeneous cloud throughout the room, the dust concentration in the cloud is:

$$c = \rho_{bulk} \left( \frac{h}{H} \right) \quad (1-2)$$

If a dust layer of thickness  $h$  on the internal wall of a cylindrical duct of a diameter  $D$  is dispersed homogeneously over the whole tube cross-section, the dust concentration is:

$$c = \rho_{bulk} \left( \frac{4h}{D} \right) \quad (1-3)$$

### 1.2.6 Ignition sources that can ignite dust clouds

Eckhoff (2003) lists some common types of heat sources that can ignite an explosible dust clouds:

- Smouldering or burning dust.
- Open flames (welding, cutting, matches, etc.).
- Hot surfaces (hot bearings, dryers, heaters, etc.).
- Electrical discharges and arcs.

Some potential ignition sources are:

- Laser light.
- Adiabatic compression and shock waves.
- Ultrasonic waves.

Scholl (1989, referred by Eckhoff, 2003) distinguished between two categories of ignition sources:

1. *Organizational* ignition sources, which can largely be prevented by enforcing adequate working routines, include:

- Smoking.
  - Open flames.
  - Open light (bulbs).
  - Welding (gas/electric).
  - Cutting (gas/rotating disc).
  - Grinding.
2. *Operational* ignition sources arise within the process itself and include:
- Open flames.
  - Hot surfaces.
  - Self-heating and smouldering nests.
  - Exothermic decomposition.
  - Heat from mechanical impact between solid bodies (metal sparks/hot spots).
  - Exothermic decomposition of dust via mechanical impact.
  - Electric sparks/arcs, electrostatic discharges.

The present thesis is concerned with ignition of dust clouds by capacitive electrostatic sparks in industrial situations. The ignition sensitivity of the dust clouds in the present thesis is measured through minimum ignition energy (MIE). A brief introduction to this research topic is presented in Section 1.4.

### 1.2.7 Means of preventing and mitigating dust explosions in the process industries

The preventive means can be split in two categories: prevention of ignition sources and prevention of an explosible dust cloud. The overview of common prevention and mitigation means are stated in Table 1-2.

**Table 1-2: Means for preventing and mitigating dust explosions in the process industries. From Eckhoff (2003).**

Prevention		Mitigation
Preventing ignition sources	Preventing explosible dust clouds	
a. Smoldering combustion in dust, dust flames	f. Inerting by N <sub>2</sub> , CO <sub>2</sub> , and rare gases	j. Partial inerting by inert gas
b. Other types of open flames (e.g. hot work)	g. Intrinsic inerting	k. Isolation (sectioning)
c. Hot surfaces	h. Inerting by adding inert dust	l. Venting
d. Electric sparks and arcs, electrostatic discharges	i. Dust concentration outside explosible range	m. Pressure-resistant construction
e. Heat from mechanical impact (metal sparks and hot spots)		n. Automatic suppression
		o. Good housekeeping (dust removal, cleaning)

With reference to Table 1-2 it is important to emphasize that most process plants can be protected against hazardous dust explosions by choosing different overall strategies for prevention and mitigation. This is illustrated in Figures 1-8 and 1-9,

using as an example a process for milling and drying of coal. Whenever a solution is developed for a given process plant, cost effective safety solutions will be an important concern.

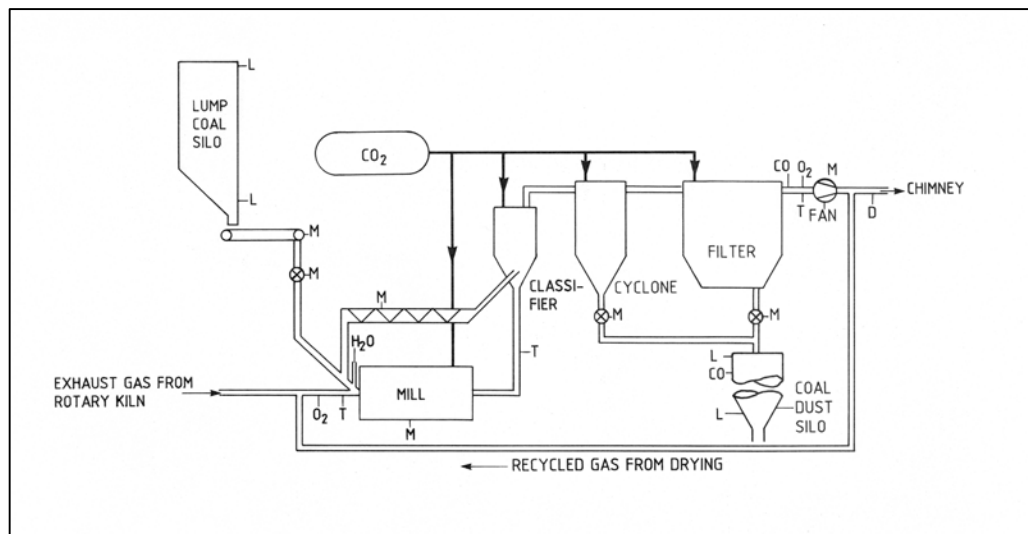


**Figure 1-8 Comprehensive sensor system for monitoring, controlling and interlocking of a process for milling and drying of coal. Explosion protection based on inerting with CO<sub>2</sub>. From Eckhoff (2003).**

CO = Carbon monoxide concentration sensors.

D = Dust concentration sensor.

L = Level sensors for coal and coal dust in silos.

M = Movement sensors for mechanical components.

O<sub>2</sub> = Oxygen concentration sensors.

T = Temperature sensors

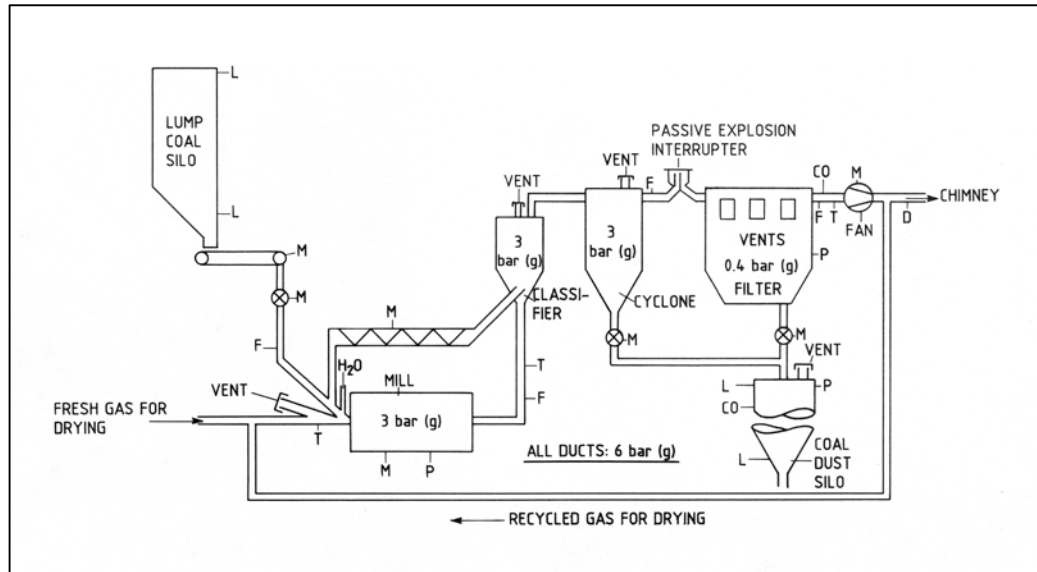


**Figure 1-9: Comprehensive sensor system for monitoring, controlling and interlocking of a process for milling and drying of coal. Explosion protection based on venting and explosion shock resistant design. From Eckhoff (2003).**

CO = Carbon monoxide concentration sensors.

D = Dust concentration sensor.

F = Flame sensor.

L = Level sensors for coal and coal dust in silos.

M = Movement sensors for mechanical components.

P = Pressure sensors.

T = Temperature sensors.

### 1.3 Case history of catastrophic industrial dust explosion in China in 2014

#### 1.3.1 Overview

The following summary is based on the paper by Li et al. (2016). On August 2, 2014, a catastrophic dust explosion occurred in a large industrial plant in Kunshan, China. The explosion occurred during manual polishing of aluminium-alloy wheel hubs for the car industry. About 75 people lost their lives immediately and 185 were injured. Subsequently, more than 71 of seriously injured also died which increased the total loss of lives to 146. The financial loss was about 350 million yuan. This is probably the most serious dust explosion catastrophe in human history apart from major coal dust explosion disasters in coal mines.

#### 1.3.2 The plant that was struck by the explosion

The explosion occurred in a two-storey reinforced concrete-frame-structure process building of length 44 m (from north to south) and width 24 m (from east to west). The two storeys comprised a basement with concrete floor and a first floor



above it. The total floor area was 2112 m<sup>2</sup>. The two floors were connected by open stair cases at each end of the building. On both sides of the eastern wall there was a 4 m by 4 m steel-panel sliding door leading to the outside.

### ***1.3.3 Process equipment layout***

The 32 polishing production lines (16 lines on the basement and 16 lines on the first floor) were arranged in parallel in the south-north direction. Along each line were 12 working stations.

On the day of the accident, 29 of the 32 production lines were in operation. 348 workers were on duty. Polishing operations were conducted manually as shown in Figure 1-10. Electric grinding guns were the main tools. According to the surface smoothness required different grades of grinding heads and/or emery papers were used.



**Figure 1-10: Workers on duty at the work stations. From Li et al. (2016).**

### ***1.3.4 Dust collection system and processing equipment***

As reported, a total of 8 sets of similar dust collection systems served all the polishing process lines on the two floors, each dust extraction system collecting the dust from 48 single work stations. According to the design of the bag filters in the dust collectors the bags were supposed to be cleaned by automatic shaking at intervals. However, after the explosion accident survivors told that, due to breakdown of the driving electric motor of the shaking system, it had been out of operation for a long time. Instead workers had cleaned the bags manually every morning before starting to work, by shaking the bags manually. This process was called "shaking ash".

The air flow for each of the 8 main dust extraction lines was produced by a suction fan mounted on the clean side of each bag filter unit. All the 8 clean-air flows from the 8 filters were joined in one main discharge duct leading to the outdoor atmosphere.

The dust explosion hazard had not been a significant concern in this kind of industry. For example, no special requirements addressing a possible dust explosion hazard had been enforced when selecting and installing the electrical equipment used

in the plant. Neither the dust collectors and the dust extraction ducting, nor all electrical sockets and power distribution cabinets had been adequately earthed.

### ***1.3.5 Explosion development***

A series of strong explosions occurred in the morning when normal hub polishing activity had been going on for about half an hour. A survivor told that he was polishing his second hub that day at the moment of the first explosion.

A video camera located outside another factory building about 500 m away from the building that exploded recorded a sequence of several explosions that lasted for about 5 to 7 s, including a distinct series of 8 successive explosions. These 8 explosions could be identified on the video recording as violent “mushroom-shaped” dust/smoke clouds being expelled abruptly from each of the 8 dust collectors.

All the windows in the first floor of the building that exploded were shattered and blown to the outside, and the window frames were completely deformed. Two-thirds of the southern wall of the building collapsed. Window frames were blown out of the eastern wall, and two air conditioners located at this wall got partly detached from the wall. The blasts also lifted some of the steel roof above the second floor, and broke all the windows. Almost all process equipment in the workshop was destroyed. Figure 1-11 shows the total damage of the process lines on the second floor.



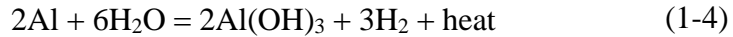
**Figure 1-11: Destroyed process lines on the second floor. From Li et al. (2016).**

### ***1.3.6 Probable ignition source of the initial primary explosion***

The investigation after the explosion revealed that the dust collecting barrel of the filter unit that suffered the first of the 8 explosions recorded by the video camera, had its bottom completely blown out. The most important observation was a small hole in this barrel wall, which was probably not caused by the explosion, but rather by corrosion over a long period prior to the explosion. Both the filters and the dust collecting barrels underneath them were located outdoors. It had been raining heavily for two days before the explosion accident, and it still rained lightly at the time of the

explosion. The investigators assumed that water had for some time entered the barrel through the corroded hole and moistened the aluminium-alloy dust inside the barrel.

This water probably was a decisive factor in the process leading to self-ignition of the contaminated aluminium-alloy dust in the barrel according to the reaction equation:



## 1.4 Specific research topic of present thesis

### 1.4.1 Introduction

The specific research topic of the present thesis belongs to the fourth item in the first column of Table 1-2 (Section 1.2.7), i.e. it is part of the wider area of preventing explosible dust clouds from being accidentally ignited by electrostatic sparks and arcs.

It has been known for more than 100 years that electric spark discharges can initiate dust explosions. As discussed by Eckhoff (2003, 2005a) the minimum electric spark energy required for ignition varies with the type of dust, the particle size distribution in the dust cloud, any moisture content in the dust, the dust concentration and the dust cloud turbulence. Furthermore, the spatial and temporal distribution of the energy in the spark is an important parameter. For many decades, it was thought that the lowest electric spark energies needed for igniting the most sensitive dust clouds in air were generally much higher, by one or two orders of magnitude, than the typical range of minimum ignition energies for gases and vapours in air. However, since 1970 it has been generally accepted that clouds in air of many dusts can be ignited by spark energies in the range of 1–10 mJ, and with some sensitive dusts can be ignited even in the range of 0.01–1 mJ i.e. the range typical of minimum ignition energies of many gases and vapours in air. According to Eckhoff (2003) the very low value of 0.01 mJ was found for a fine sulphur dust by Bartknecht (1993).

### 1.4.2 Electric/electrostatic spark discharges

One often distinguishes between *inductive (break flash)* and *capacitive* electric spark discharges. Inductive (break flash) sparks are generated when live electric circuits are suddenly broken. The energy discharged is then the energy stored in the inductance  $E_L$ , neglecting external circuit losses, is:

$$E_L = \frac{1}{2} Li^2 \quad (1-1)$$

Here  $E_L$  is the stored energy in inductor in joule,  $L$  is inductance in henry and  $I$  is current in ampere. However, the discharge type of concern in the present study is capacitive electrostatic spark discharges. They occur when electrostatic charge that has accumulated on an electrically conducting, unearthed, object (i.e. an electric capacitance) e.g. a silo, is discharged to earth across an air gap of suitable length. In process industries that produce and/or handle powders, electrostatic charging is generally tribo-electric. This implies that electrons are transferred between two objects of different electron affinity when the objects are separated after having first

been in contact. In a process plant this can occur during handling (Glor, 1988) and transport of powder and dust whenever powder/dust and process equipment make contact and are subsequently separated. This charging mechanism can be comparatively slow, and to explain the simultaneous occurrence of an accidental spark discharge and an explosible dust cloud in the area of the spark, some synchronization mechanism must be sought.

Another, much faster charging mechanism can operate in bag filters that are cleaned automatically at intervals by a pulse of compressed air released on the clean side of the filter. A central condition for this type of discharge to occur is that there is some non-earthed metal component on/in the filter that can be charged triboelectrically by the rapid passage across this component of the dust released in the cleaning process. A second condition is that in the area where the dust cloud appears there is also a spark gap of suitable length across which a spark can jump. A third condition is that the stored electrical energy on the charged conducting component  $E_C$  is sufficient for the spark discharge to be able to ignite the dust cloud under the prevailing turbulent conditions.

In both these cases the energy available for the discharge is:

$$E_C = \frac{1}{2} CV^2 \quad (1-2)$$

Here  $E_C$  is the stored energy in the capacitor in joule,  $C$  is capacitance in farad and  $V$  is voltage in volt. The present thesis focuses on a different practical situation where electrostatic capacitive spark discharges between two electrically conducting electrodes may occur, but *where the charge build-up is rather slow*. The key question is then: How is synchronization between spark discharge and dust cloud appearance brought about?

A possible practical industrial situation where this may occur is illustrated in Figure 1-12.

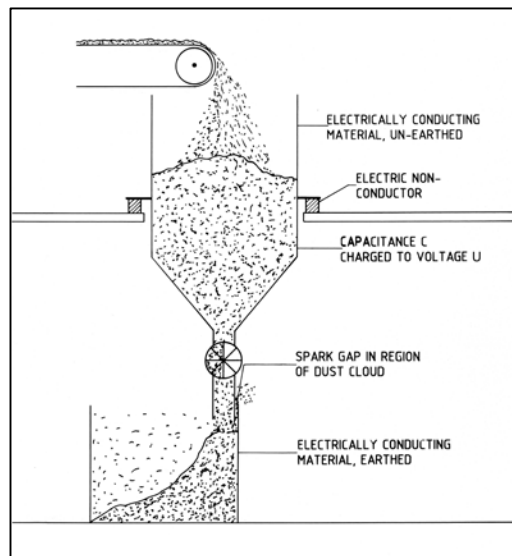


**Figure 1-12: Illustration of practical situation spark discharge situation in focus in the present study. From Eckhoff (2003).**

Here an unearthed metal silo is being filled with an electrostatically charged powder that has been dropped into the silo from a belt conveyor. One mechanism by which the silo body can be charged in the situation sketched in Figure 1-12 is electrostatic influence from the charged powder in the silo. The mechanism is then that charge on the powder particles induces displacement of the electrons in the electrically neutral metal silo, which may, if circumstances are favourable for this, give rise to a high-voltage across the potential spark gap. However, depending on the electrical conductivity of the particles in the silo, charge may also migrate directly from the powder to the silo walls.

If, in some place, the silo body is separated from earth by only a small gap of the order of only a few millimeters, a spark discharge may occur across this gap if a sufficiently high-voltage has been allowed to build up on the silo.

An important issue is then whether there will be an explosible dust cloud at the location of the sparks gap just at the moment of spark discharge. One possible mechanism was found nearly 50 years ago by Eckhoff (1970). He observed that a capacitive spark gap, across which the voltage was slightly lower than the natural breakdown voltage in air, could be broken down by blowing a dust cloud into the gap region. He subsequently used this simple synchronization mechanism in his electric spark ignition experiments with clouds of lycopodium dust in air.

Clearly, this type of spark gap breakdown also constitutes a plausible mechanism by which the appearance of an explosible dust cloud at a potential spark gap carrying a high-voltage, can initiate a synchronized spark discharge across the gap and give rise to an accidental dust explosion. Randeberg and Eckhoff (2004) and Eckhoff and Randeberg (2005b) also pointed out that this may be a mechanism by which combustible dust clouds in industrial plant may trigger and get ignited by accidental electrostatic spark discharges.

## **2 Review of literature related to the specific topic of the present thesis**

### **2.1 Experimental studies of electric spark gap breakdown by dust particles**

#### **2.1.1 Investigation by Eckhoff (1970)**

This Section is to a large extent based on the recent paper by Eckhoff (2016).

A vertical cross-section of the explosion vessel used by Eckhoff (1970) is shown in Figure 2-1. It was a cylindrical brass vessel of 1 litre volume and internal diameter of 100 mm. The horizontal cross-section showing the electrode arrangement is given in Figure 2-2.

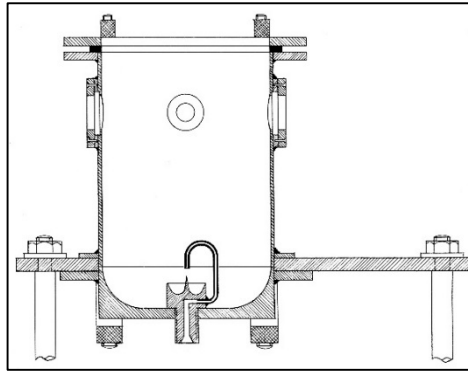


**Figure 2-1: Vertical cross-section of explosion vessel showing dust dispersion cup at vessel bottom. As indicated by two concentric circles the electrodes were perpendicular to the sectioning plane in the upper part of the vessel. From Eckhoff (2016).**

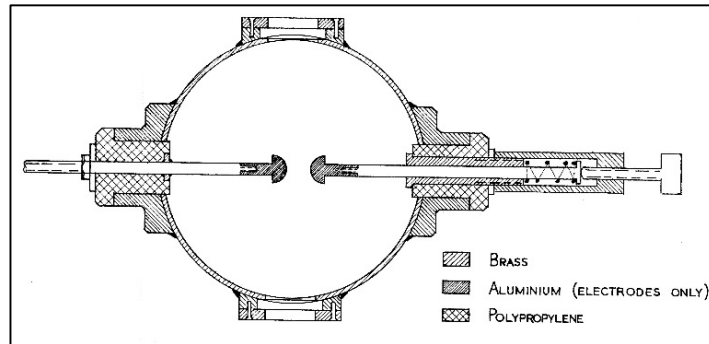


**Figure 2-2: Horizontal cross-section through electrode system and glass windows for viewing electrode gap. From Eckhoff (2016).**

In explosion experiments the top of the vessel was covered by a filter paper to ensure adequate explosion venting. The spark electrodes were two 10 mm diameter aluminium hemispherical. The high-voltage electrode was fixed, whereas the earthed electrode was threaded to allow adjustment of the spark gap length as shown in Figure 2-2. The transient dust clouds for the explosion experiments were obtained by dispersing a given mass of lycopodium placed in the dust dispersion cup also shown in Figure 2-1.

The electric spark discharge circuit was a simple RCL circuit. A detailed wiring diagram is given in Eckhoff (2016). The small inherent circuit inductance was 2-3  $\mu\text{H}$ , and the minute external circuit resistance only about 0.01  $\Omega$ . The resistances of the sparks were of the order of 1  $\Omega$ , decreasing somewhat with increasing spark energy. Typical spark discharge times were about 5  $\mu\text{s}$ . The spark energy ranges investigated, in terms of  $\frac{1}{2}CV^2$ , was 0.85-8.5 J.

Synchronization of the appearance of the transient dust cloud and the spark discharge was accomplished by initiating the spark discharge by the dust cloud itself when its front entered the spark gap. To accomplish this, the voltage across the spark gap had been pre-set at about 0.2 kV below the natural breakdown voltage of the gap in the absence of dust, which was about 10.0 kV for the 2.66 mm gap used in most of the experiments.

The experimental results for a given spark energy was plotted in terms of the probability of ignition as a function of the nominal dust concentration (mass of dust dispersed divided by the volume of the explosion vessel). The gross probabilities of ignition were based on the outcomes of 100 experiments at the same spark energy and nominal dust concentration. For practical reasons, the 100 experiments were conducted in five consecutive batches of 20 experiments each. Figure 2-3 gives a typical set of results.

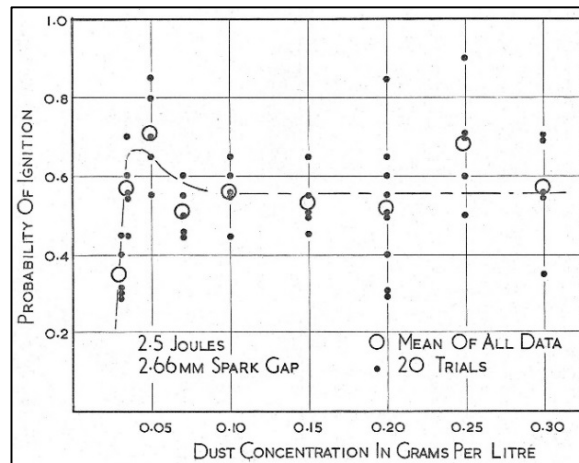


**Figure 2-3: Experimental results with 2.5 J spark energy and spark gap length 2.66 mm. From Eckhoff (1970, 2016).**

The small black dots in Figure 2-3 are the results based on batches of 20 successive experiments. The large open circles are the gross result from five successive batches of 20 experiments. The experimental probabilities of ignition are plotted as a function of the nominal dust concentration. A significant feature of Figure 2-3, and of all the experiments performed by Eckhoff (1970) was that all the gross probabilities  $P$  of ignition were  $0\% < P < 100\%$  in spite of the comparatively very large spark energies used. Published evidence suggesting a plausible physical reason for this is reviewed in the following Section 2.2.

Randeberg and Eckhoff (2004, 2006a) and Eckhoff and Randeberg (2005b) determined the MIEs of three dusts (lycopodium clavatum, sulphur and maize starch) using the dust cloud spark gap breakdown method. The MIEs obtained were somewhat higher than, but of the same order as, those obtained using conventional methods with special dust cloud/spark discharge synchronization systems. This was believed to be due to non-optimal delay for ignition between dust dispersion and onset and spark breakdown in the case of dust cloud triggering of the spark discharge. This means that neither dust the concentration nor the dust cloud turbulence at the moment of sparking were optimal for ignition.

On the other hand, the inherent spark triggering process is probably in closer agreement with the electrostatic spark triggering mechanisms operating in industrial accidental ignition situations.

## 2.2 Influence of spark discharge time on MIE of dust clouds

It has been known for more than half a century that the discharge times of capacitive electric sparks can influence the MIE of dust clouds substantially. The pioneering contributions by Boyle and Llewellyn (1950) and Line et al. (1959) then have to be emphasized. They showed by independent experiments that net minimum capacitive-electric-spark energies for igniting explosive clouds in air of both organic and metal dusts were reduced by a factor of up to 100 when spark discharge times were increased from a few microseconds to 0.1-1 ms.

Boyle and Llewellyn (1950) used transient dust clouds of quite short life time in their experiments. Synchronization between the appearance of the dust cloud in the region of the spark gap and the spark discharge was obtained by using a movable earthed electrode. Before an experiment the electrode spacing was kept much larger than the small distance required for spark-over at the prevailing high-voltage. However, at the same time as the air blast that dispersed the dust into a cloud was activated, the earthed electrode was rapidly displaced to produce a sufficiently small spark gap for the spark discharge to occur. Figure 2-4 shows some experimental results for  $< 76 \mu\text{m}$  fractions of Al and Mg dusts. The following conclusions can be drawn from Figure 2-4.

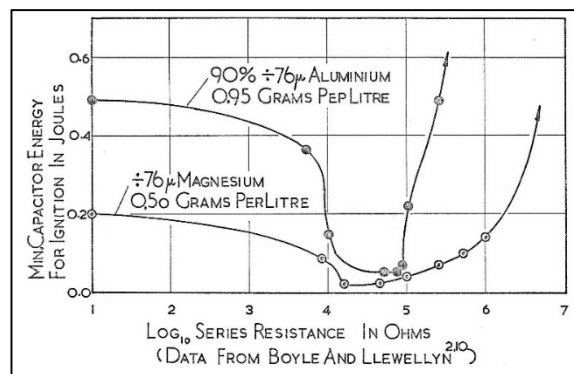


**Figure 2-4: Experimental minimum ignition energies for clouds in air of dust of aluminium and magnesium. From Boyle and Llewellyn (1950).**

With a series resistance of 10-100 k $\Omega$  in the spark discharge circuit, the stored capacitor energy  $\frac{1}{2} CV^2$  required for ignition was reduced by factors of about 10, even though, as shown by the data in Figure 2-5, about 90 % of the energy originally stored in the capacitor was absorbed by the external resistance.



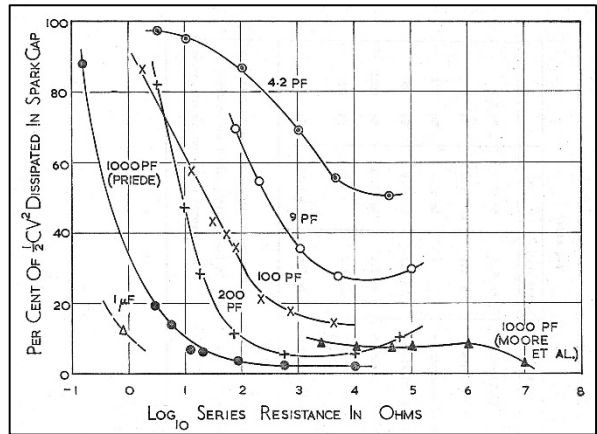


**Figure 2-5: Percent of discharge capacitor energy actually delivered to the spark gap in capacitive discharges containing an external series resistance. From Priede (1958) and Moore et al. (1956).**

This means that under these circumstances the net spark energy required for ignition was only about 1% of the net spark energy required with no added series resistance. There is little doubt about this was because the large added series resistance increased the time constant  $R \cdot C$  of the discharge dramatically, and hence reduced the shock wave disturbance of the dust cloud by the spark discharge correspondingly.

Line et al. (1959) studied capacitive-electric-spark ignition of about 25 mm diameter columns of settling clouds of *lycopodium* dust in air. Some of their results are shown in Figure 2-6.

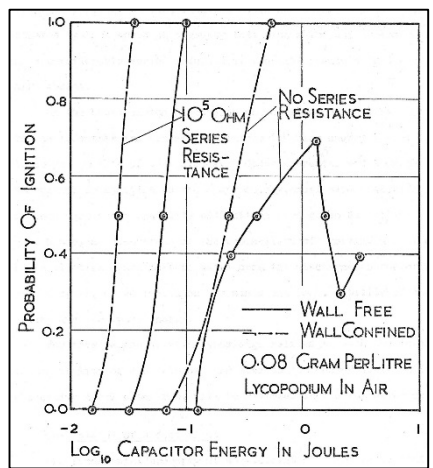


**Figure 2-6: Experimental minimum ignition energies for lycopodium dust in air. From Line et al. (1959).**

The dust columns were either “wall-free” or confined inside a vertical glass tube (“wall-confined”). The results given in Figure 2-7 confirm the results in Figure 2-5. Again the inclusion of a 100 k $\Omega$  series resistance reduced the gross capacitor energy for ignition appreciably, and the net spark energy for ignition was again reduced by a factor of 50-100 (Figure 2-6). Furthermore, with “wall-free” dust columns and no

series resistance the probability of ignition did not increase monotonically with the capacitor energy, but in fact dropped with increasing capacitor energies in the range  $> 1$  J.

In the “wall-free” case, using high speed camera, Line et al. (1959) also demonstrated experimentally that with no series resistance the shock waves emitted by spark discharges of energies of the order of 1 J effectively pushed the dust particles away from the spark. This, for some time interval, interrupted the contact between the spark channel and the dust particles and ignition was prohibited. This effect disappeared when a series resistance of 100 k $\Omega$  was inserted into the discharge circuit. The same happened when the spark discharge time was prolonged by including a comparatively large series inductance in the discharge circuit.

Eckhoff (1970, 2016) described this effect as illustrated in Figure 2-7.

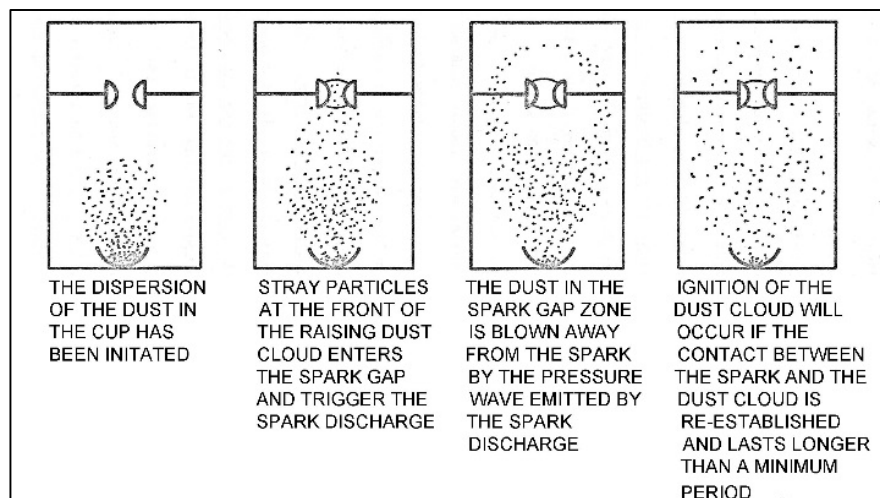


**Figure 2-7: Qualitative conception of dust cloud ignition process with strong electric sparks of short discharge times. From Eckhoff (1970, 2016).**

According to Figure 2-7 the process of ignition of transient dust clouds by strong electric sparks of short discharge times comprises 4 consecutive stages. In stage 1 the dispersing air blast has started to raise the dust into a cloud, which expands towards the region of the spark gap in the upper part of the bomb. The voltage across the spark gap has in advance been set at a level slightly below the natural breakdown voltage in air only. In stage 2 the front of the raising dust cloud arrives at the spark gap, causing gap break-down and formation of the spark channel. In stage 3 the dust in the vicinity of the spark is pushed away by the shock/blast wave emitted from the highly pressurized spark channel, leaving a dust free zone round the spark. In the final stage 4 the crucial question is whether the dust cloud is capable of recovering from the disturbance in time, so that contact between the spark channel and the dust can be re-established for a sufficiently long time to allow ignition to take place (Eckhoff, 1970).

Eckhoff (1970, 2016) also put forward a highly tentative, mostly empirical mathematical model that was able to predict the probabilities of ignition obtained in his experiments. He suggested that three key time parameters must be considered:

- The duration of the spark channel the time elapsed from the breakdown of the spark gap till the temperature in the spark channel has decreased below the minimum level necessary for ignition.
- The minimum time of contact between dust cloud and spark, required for ignition of the dust cloud. It was assumed that this minimum time of contact depends upon both the spark energy and an inherent “combustibility” parameter of the dust cloud, defined by Eckhoff (1970, 2016).
- The statistical distribution of the time interval from breakdown of spark gap till re-establishment of contact between spark channel and dust cloud. Eckhoff suggested that this distribution constitutes the stochastic element in this type of experiment.

The dust “pushing” effect of shock waves from spark discharges, as observed by Line et al. (1959), was later studied experimentally by Eckhoff and Enstad (1976). However, instead of dust particles they used a small 5 mm • 4 mm piece of very thin paper hanging close to the spark gap, supported by two very thin threads. The set-up is illustrated in Figure 2.8. With a spark energy of 0.3 J and 1  $\mu$ s discharge time, the paper piece was pushed 35 mm to the side of the spark, whereas with 0.3 J and about 100  $\mu$ s discharge time, this distance was only about 1 mm.

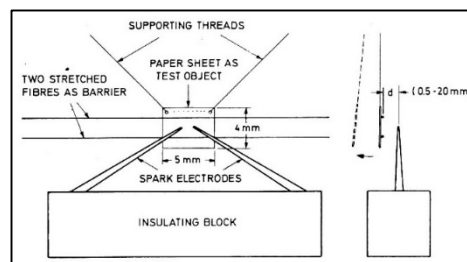


**Figure 2-8: Experiment for studying the disturbance effect of shock wave from spark discharges. From Eckhoff and Enstad (1976).**

As reviewed by Eckhoff (2003), Enstad (1981) performed a comprehensive theoretical analysis of the ability of the shock wave emitted from a 1.5 J spark discharge of very short discharge time, to displace lycopodium dust particles at various initial distances from the spark. The theoretical analysis confirmed the formation of a dust free zone surrounding the spark channel, as illustrated in Figure 2.9

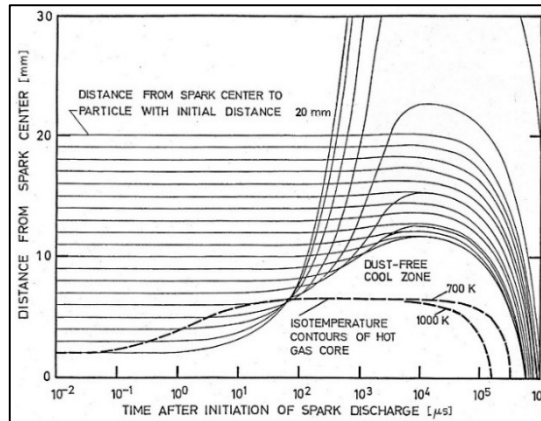


**Figure 2-9: Theoretically predicted displacement of dust particles at various initial distances away from a 1.5 J spark discharge as a function of time. From Enstad (1981).**

### 2.3 Theory on electrical circuits

An electrical circuit comprises three main parts, viz. a source, a load and a path. If an electric current is flowing in the circuit, it is denoted *closed*, if no current is flowing, it is denoted *open* (Matt, 2013).

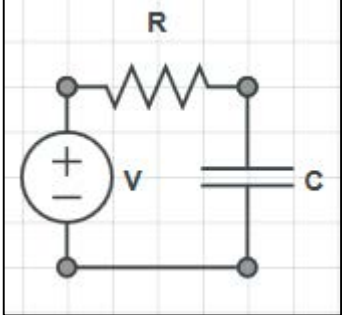
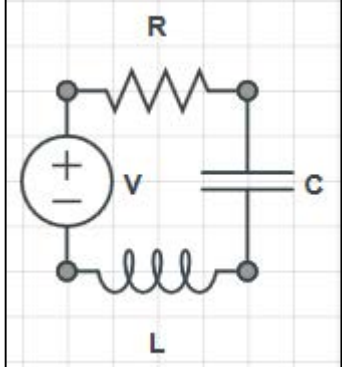
The standard electrical units related to the work presented in the present thesis are given in Table 2-1.

**Table 2-1: Standard electrical units**

Electrical variable	Variable symbol	Measuring unit / symbol	
Capacitance	$C$	Farad	F
Charge	$Q$	Coulomb	C
Current	$I$	Ampere	A
Inductance	$L$	Henry	H
Resistance	$R$	Ohm	$\Omega$
Voltage	$V$	Volt	V

In the context of the present thesis, RC and RCL *series* circuits are generated when tribo-electrically generated electrostatic charge is suddenly released as a spark discharge from a capacitance  $C$  to earth, either via just a resistance  $R$ , or via an  $R$  and an inductance  $L$  in series. The spark gap then essentially constitutes part of the resistance. The components and equivalent circuit of RC and RCL series circuits are illustrated in Table 2-2.

**Table 2-2: RC and RCL series circuits**

Electrical circuit	Components	Equivalent circuit
RC	Resistor ( $R$ ) Capacitor ( $C$ )	
RCL	Resistor ( $R$ ) Capacitor ( $C$ ) Inductor ( $L$ )	

As has already been discussed above, it is not only the stored energy on the capacitor that determines whether ignition of a dust cloud by a spark discharge will occur or not. The duration of the spark discharge is also of great importance. The time constant ( $\tau$ ) of a spark discharge is defined as the time required for the amplitude of the spark current to drop to 37% of the initial value. The time constant for an RC circuit is:

$$\tau = R \times C \quad (2-1)$$

The time constant for RCL circuit is:

$$\tau = \frac{2L}{R} \quad (2-2)$$

In practice an electrical circuit will always contain an inherent circuit inductance, although small in some cases, which means that equation 2-2 applies. The decaying oscillation of spark current and voltage in time during a spark discharge is known as *damping response*. The cause of damping is due to the resistance. One distinguishes between three possible damping responses, viz. *overdamped*, *critically damped* and *underdamped*. The three cases are illustrated in Figure 2-10.

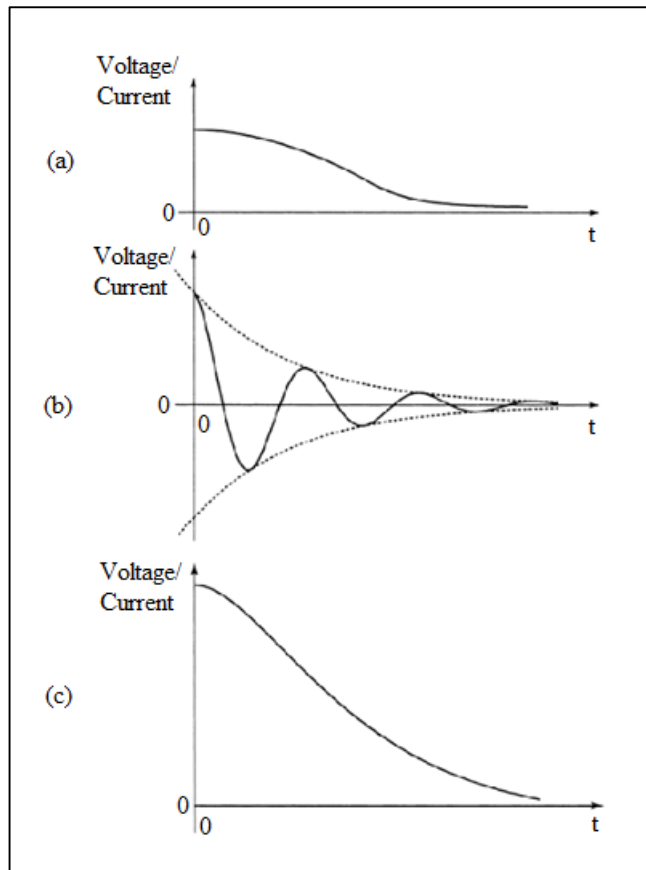


**Figure 2-10: Graph of transient response. (a) overdamped, (b) underdamped, (c) critically damped. Based from Attenborough (2003).**

In Figure 2-10, the y-axis represents both voltage and current. The behaviour of *overdamped* discharges is not oscillatory and current and voltage decay fast. For *underdamped* discharges, however, the behaviour is oscillatory, with both current and voltage decreasing exponentially. The discharge duration is somewhat longer than for the overdamped case. The behaviour of *critically* damped discharges is also not oscillatory and decays faster than in overdamped cases. According to Bourne (2016), if the values of all three components  $R$ ,  $C$  and  $L$  are known, damping can be identified through the mathematical relationships of  $R$ ,  $C$  and  $L$ . This is illustrated in Table 2-3.

**Table 2-3: Mathematical equations of damping response through of  $RLC$  relationships according to Bourne (2016).**

Damping	Mathematical equation
Overdamped	$R^2 > \frac{4L}{C}$
Underdamped	$R^2 < \frac{4L}{C}$
Critically damped	$R^2 = \frac{4L}{C}$

Another mathematical expression that can identify damping response is from the Kirchoff's voltage law. This is illustrated in Table 2-4.

**Table 2-4: Application of Kirchoff's voltage law for RC and RCL series circuit**

Series electrical circuit	Equivalent mathematical equation
RC	$RI + \frac{Q}{C} = 0$
RCL	$RI + \frac{Q}{C} + L \frac{di}{dt} = 0$

According to Attenborough (2003), damping response can also be described mathematically by differentiating the equations listed in Table 2-4. The differentiated equation forms a second order linear homogeneous equation. The second order linear equation is:

$$y(t) = ax'' + bx' + cx \quad (2-3)$$

The quadratic equation is:

$$x_1, x_2 = \frac{-b \pm \sqrt{b^2 - 4ac}}{2a} \quad (2-4)$$

Equation 2-4 has three are three possible of equivalent roots:

1. Distinct roots where  $x_1 \neq x_2$ . In this case the system is overdamped. Thus the general solution is  $y(t) = Ae^{x_1t} + Be^{x_2t}$ .
2. Roots are equal,  $x_1 = x_2$ . In this case the system is critically damped. Thus the general solution is  $y(t) = (A + Bt)e^{xt}$ .
3. Roots are complex,  $\alpha \pm \beta i$  or  $\alpha \pm j\omega$ . In this case the system is underdamped. Thus the general solution is  $y(t) = e^{-\alpha t} (A \cos \omega t + B \sin \omega t)$ .

Here  $\alpha$  is the damping coefficient,  $\omega$  is the angular resonant frequency. As pointed out by Attenborough (2003) the function decays to zero as  $t \rightarrow \infty$  as the energy in the circuit is vanishing in heat.

## 2.4 Breakdown voltage mechanism in the air between two conducting electrodes

The dielectric strength of an insulating material between two conductive electrodes can be broken down if the voltage across the electrodes exceeds a certain limit. The dielectric medium between the two electrodes can be air, as in the present case, or any other electrically insulating material. Breakdown voltage in air between the two electrodes starts with an avalanche of electrons being released from the negative

electrode (cathode) and heading at high speed towards the positive electrode (anode) or simply known as “ionization”. On their way towards the anode the electrons collide with oxygen and nitrogen molecules, which are then transformed into conductive ions. In this way an electrically conducting channel of some resistance is established between the two electrodes, into which electricity flows through the channel. Due to the heat deposited in the channel, it can acquire both a very high temporal temperature and a very high temporal pressure (Hong, 2000). This is a spark discharge.

The critical electric field around the electrodes for the voltage breakdown in air to occur is given by the equation:

$$\varepsilon_c = \frac{V_{bd}}{d} \quad (2-4)$$

Here  $\varepsilon_c$  is the dielectric strength of air in V/m,  $V_{bd}$  is the breakdown voltage in V and  $d$  is the gap distance between the electrodes in m. As shown in Table 2-5, Hodgman (1925) listed the dielectric strength of air depending on the electrode shape. This applies to the present thesis, the estimated breakdown voltage for 2 mm electrode gap for hemispherical electrode is about 9 kV and for cylindrical flat-end electrode is about 7.4 kV if referred to pointed electrodes shown in Table 5-5 that in reality gives a small difference in terms of the tip of electrodes. The electrodes in the present thesis will be discussed further in Chapter 3.

**Table 2-5: Dielectric strength of air. From Hodgman (1925).**

Electrode type	Dielectric strength of air (V/m)
Ball electrodes, 1 cm diameter	$4.5 \times 10^6$
Pointed electrodes	$3.7 \times 10^6$

## 2.5 Breakdown voltage mechanism by dust particles between electrode gap

Dust particles in the air gap between two conductive electrodes can decrease the breakdown voltage of the gap. The reason for this is probably very complex. If the dust particles come from deposited dust blown into an airborne cloud by a blast of compressed air, the particles can get charged tribo-electrically. According to Wadha (2007), dust particles can be charged to the polarity of the electrode that they first hit, and therefore they may become attracted by the opposite electrode due to the field forces, whereby breakdown of the gap is triggered.

# 3 Experimental apparatus and methods

## 3.1 Experimental apparatus

Experimental apparatus is composed of an explosion vessel, a dust dispersion system, an electric spark discharge system, and measuring instruments. A



photographic overview is shown in Figure 3-1. The various elements will be explained in detail below.

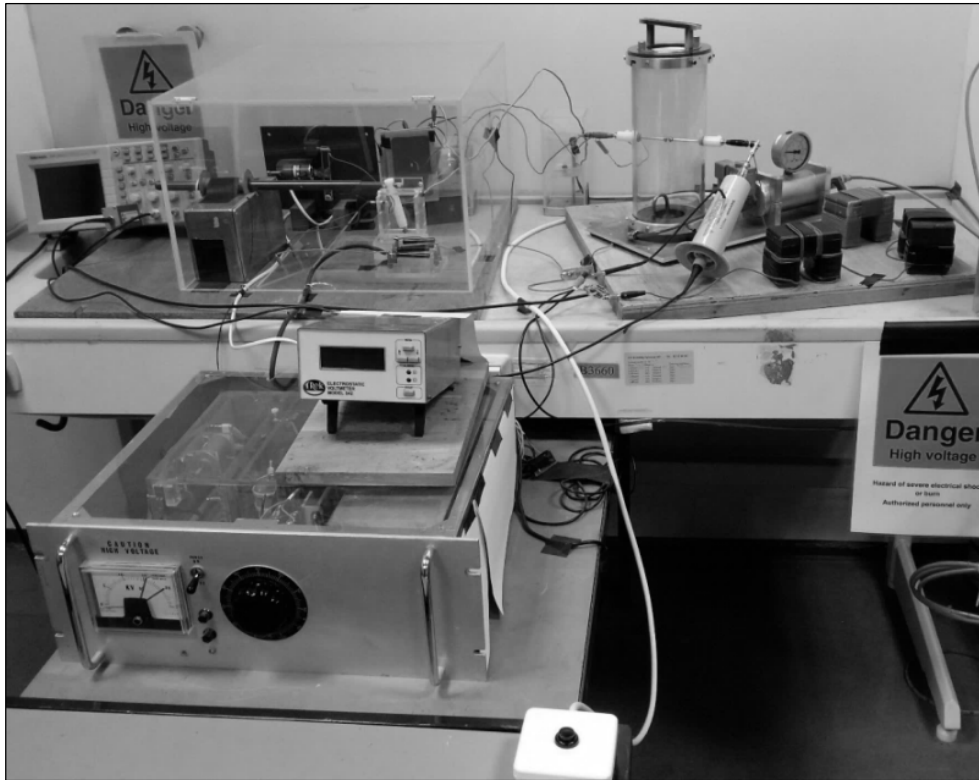


**Figure 3-1: Experimental apparatus arrangement**

### ***3.1.1 Explosion vessel***

A schematic diagram of the explosion vessel is shown in Figure 3-2. The vessel is a 2.6 liter cylindrical pipe made of transparent hard plastic, with an internal diameter of 110 mm and 5 mm wall thickness. The bottom of the vessel is made of PVC plastic and bolted to a metal plate. The top of the vessel is covered by a paper sheet clamped to the vessel by a plastic ring arrangement fixed to the top of the vessel. The dust basin is a cup containing the dust to be dispersed into a cloud is a milled, shallow basin at the centre of the bottom plate of the vessel. As shown in Figure 3-2, two electrode rods with 4 mm diameter are inserted diametrically opposite into the vessel with similar electrodes screwed on the tip of electrode rods inside the vessel to form a spark gap. The electrode rods are adjustable depending on the desired spark gap distance which can be fixed by a screw. In the present thesis, the electrodes spark gap distance is 2 mm for all experiments. The types of electrodes which are made of brass are hemispherical electrodes with 10 mm diameter and 1 mm diameter cylindrical flat-end electrodes. The two types of electrodes are shown in Figure 3-3.

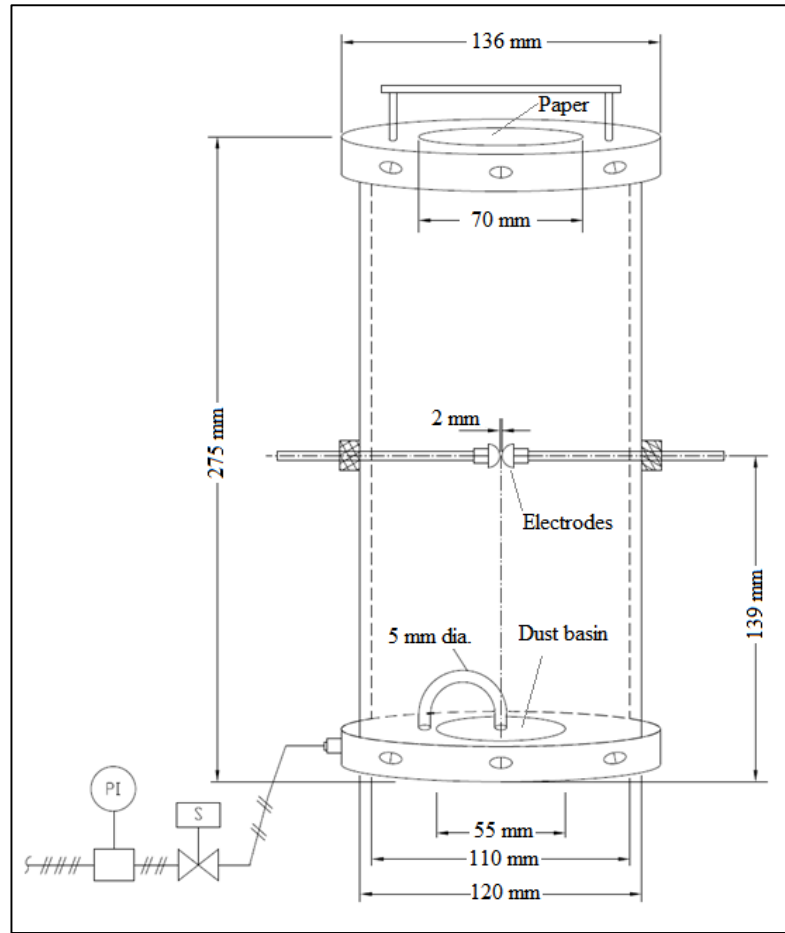


**Figure 3-2: Schematic diagram of explosion vessel.**

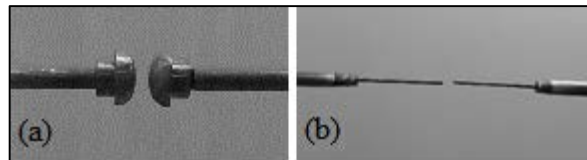


**Figure 3-3: Types of electrodes: (a). Hemispherical electrodes (10 mm  $\varnothing$ ), (b). Cylindrical flat-end electrodes (1 mm  $\varnothing$ ).**

### **3.1.2 Electric spark discharge system**

The electric spark discharge system is composed of a high-voltage power supply, passive components (resistor, capacitor and with or without inductor), a pair of similar electrodes, and equipped by measuring instruments. A spark discharge is generated between the gap of electrodes that are shown in Figures 3-2 and 3-3. High-voltage power supply is connected to the passive components in series with the electrodes. The schematic diagram of the two circuits used to generate spark discharge are shown in Figure 3-4.

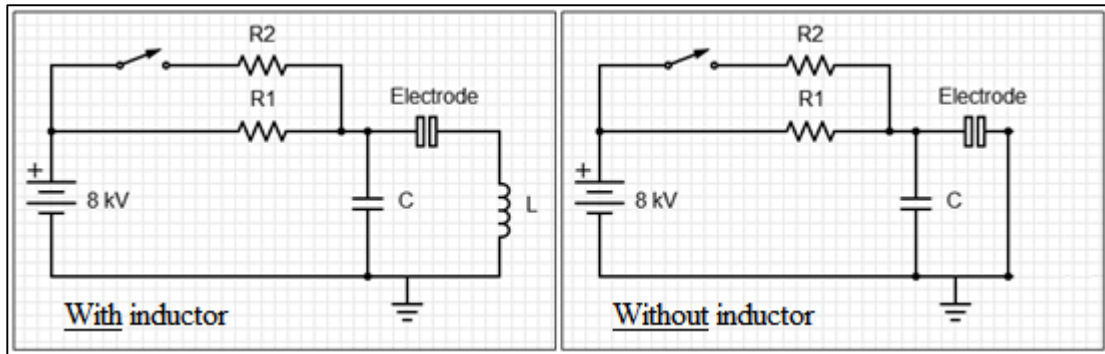


**Figure 3-4: Schematic circuit diagrams to generate a spark discharge.**

In Figure 3-4, the high-voltage capacitor  $C$  values are varied from 0.19 nF to 100 nF. A longer spark duration was obtained by additional series inductance  $L$  varied from 0.118 mH, 1.26 mH, to 2 mH in the circuit. A single experiment was also carried out with an additional series inductance of 2.4 mH. The calculated inherent inductance of the circuit without additional inductor was approximately 2  $\mu$ H.

In Figure 3-4, the main resistor  $R_1$ , varies from 800 G $\Omega$  to 1 T $\Omega$  to avoid losses in the stored energy in the capacitor and for the stability of the set supply voltage before the initiation of dust cloud. However, the charging duration was longer because of high-resistance in  $R_1$ . A “bypass” resistor  $R_2$  was connected in parallel to  $R_1$  to reduce the duration of charging that is activated by a sliding switch. Therefore, the equivalent resistance during charging was lower and the charging duration is shorter. The resistance of a bypass resistor  $R_2$  is within the range of 320 M $\Omega$  to 200 G $\Omega$  that depend on the capacitance in the circuit. Bypass resistor  $R_2$  was removed by pulling the switch to open position when the set supply voltage in the circuit was reached to determine the MIE of dust cloud. However, a bypass resistor  $R_2$  was not removed from the circuit for a continuous flow of supply voltage to the determination of actual breakdown voltage in air. The instruments connected to the circuit can monitor neither the charge nor the energy accumulated in the capacitor, but the supply voltage only. The supply voltage is either continuous or with limited range that depend on the type of electrodes used and desired spark energy. This will be discussed in Section 3.2.1.

### 3.1.3 Dust dispersion system

The dust dispersion system is through air blast that can control the dispersing air pressure. The system is composed of a cylindrical air reservoir tank, manual operated valve with pressure indicator, solenoid valve, and U-shaped tube shown in Figure 3-5.

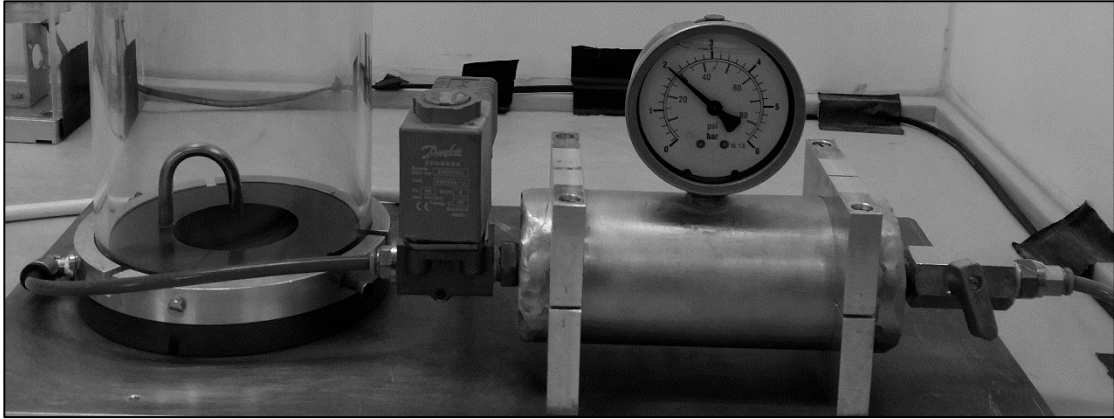


**Figure 3-5: Dust dispersion system with dust basin to the left and compressed-air on cylindrical reservoir tank for dust dispersion to the right. The solenoid valve releasing the air blast for dust dispersion is between the vessel and the cylindrical reservoir tank.**

A compressed air is stored in a cylindrical air reservoir tank of 416 cm<sup>3</sup>, equipped with pressure indicator. Air pressure is adjustable from the main air supply. Air blast is activated by an electric switch that was released through the inverted U-shaped tube with 5 mm diameter pointing at the centre of dust basin with lycopodium dust that initiate dust cloud.

#### **3.1.4 Measuring instruments**

The measuring instruments that are connected directly to electrical circuit were:

- Electrostatic voltmeter.
- Oscilloscope equipped with two probes.

The additional instruments that are not directly connected to the circuit were:

- High-speed camera
- LCR meter
- Weighing scale
- Function generator
- Tool for adjusting the electrode gap distance to a desired value.

The photographs of all the measuring instruments are shown in Appendix A.

The “Trek” model 542 electrostatic voltmeter includes sensor elements: a vibrating sphere, and a plate connected to the positive side of an electrode. Electrostatic voltmeter was used to monitor the actual voltage on the capacitor during charging, and also the actual breakdown voltage in air. The sensor elements are contained in a clear hard plastic enclosure for protection against dust. Electrostatic voltmeter measurement range is 0 to  $\pm 10$  kV DC, and the reading accuracy is 0.5 kV. Electrostatic voltmeter has a function of holding the peak voltage.

The “Tektronix” TDS 2002 oscilloscope measures the duration of spark discharges and the fast transient voltage variations across the spark gap taking place during

electric spark discharges across the gap. The oscilloscope is equipped with two probes:

1. Tektronix P6015A high-voltage probe with 20 kV DC, detecting pulses up to 40 kV, with attenuation up to 1000, and 75 MHz bandwidth.
2. An ordinary probe with or without converter to attenuate the actual measured voltage by a factor of 10 on the display of oscilloscope. This converter was particularly useful with circuits without an additional inductor. This probe was connected across a 0.1 or a 0.3  $\Omega$  resistor for current measurement.

Photron SA4 high-speed camera captured the phenomenon from dust cloud generation, electric spark discharge to the resulting ignition with timer features. The frame rate setting used varied from 3600 fps, 10,000 fps, 50,000 fps and 100,000 fps.

Portable LCR meter measures inductance, capacitance, and resistance, used for varying the values of passive components.

Weighing scale measures the mass of lycopodium dust to be dispersed through explosion vessel.

Function generator measures the high-frequency and low-frequency of the circuit to calculate the resistance of the inductors.

Tool for adjusting the electrode gap is a steel plate, 2 mm thick.

## 3.2 Methods

### 3.2.1 Electric spark discharge generation

To obtain a desired spark energy both the capacitance  $C$  and the voltage  $V$  across the spark gap has to be calculated accordingly based on equation 1-6.

Two types of spark generation circuits were used, which are with an additional series inductor, and without such an inductor. The two circuits are illustrated in Figure 3-4 in Section 3.1.2.

In both circuits the electrical energy that was initially stored in the capacitor is deposited in the spark gap during the triggered electric spark discharged. An additional inductor is connected in series with the electrode connected to the capacitor. The purpose of the inductor is to increase the duration of the spark discharge. The energy delivered to the spark, decays with time until the discharge eventually extinguishes. In order to study the electric spark discharges more closely, they were initiated in two ways:

1. By raising the supply voltage continuously until the actual breakdown voltage occurred without a dust cloud across the spark gap by 10 repeated test each conditions.
2. By raising the supply voltage to a level lower than the actual breakdown voltage in air, then breakdown occurs between the gap by dispersing a dust cloud into it. The set supply voltage for hemispherical electrodes are 8 kV and for cylindrical flat-end electrodes are 4.5 kV.

The supply voltage in the capacitor is monitored by a voltmeter connected on the positive side of the electrode. Oscilloscope is connected on the negative side of the electrode which is triggered when electric spark is discharged. After electric spark discharged is generated either with or without ignition, high-voltage power supply is

turned off. For safety purposes, which is not part of electric spark discharged generation, a relay is attached on the switch of high-voltage power supply which is not shown in Figure 3-4. A relay will open when a high-voltage power supply switch is turned “on” and closes when high-voltage power supply is turned “off” to fully discharge the remaining energy in the capacitor after each tests.

At charging period, bypass resistor is switched on continuously for item 1 only. For item 2, a bypass resistor is switched off when the set supply voltage is reached, then the energy stored is stabilized because of high-resistance of the main resistor. Then dust cloud generation system is activated. The released dust cloud is charged through tribo-electric charge, and create a path between the electrode gap, and a breakdown resulting to electric spark discharge. Additional resistor is connected in series next to inductor, the resistor value is  $0.1 \Omega$  to  $0.3 \Omega$  to measure the current.

### ***3.2.2 Dust dispersion system***

Lycopodium dust of nominal concentration is placed on the dust basin, followed by securing the explosion vessel on the base. Majority of the dispersing air pressure was 1 bar and for additional tests were varied from 3 bar to 3.5 bar. Then air blast is activated by a manual switch to release the air through the inverted 5 mm U-shaped tube pointing directly on the centre of dust basin creating a dust cloud.

### ***3.2.3 Determination of MIE***

The early phase of testing was performed by 100 repeated tests conditions, then revised to 40 repeated tests on the succeeding conditions to determine MIE. The energy stored in the capacitor start from highest to the lowest energy until no ignition is observed.

For hemispherical electrode, the stored energy varied from 3200 mJ to 6 mJ. The conditions for each set of energies are with four different spark discharge duration by changing the inductance to 0.118 mH, 1.26 mH, 2 mH and without inductance that is only used for energy below 256 mJ.

For cylindrical flat-end electrode, stored energy varied from 10 mJ to 6 mJ because of the time frame needed to complete the research. The conditions for each set of energies are with three different spark discharge duration by changing the inductance to 0.118 mH, 1.26 mH and 2 mH only because of unstable and sensitive condition of cylindrical flat-end electrode.

The following steps are performed for the determination of MIE of transient lycopodium dust cloud:

1. Nominal stoichiometric concentration of lycopodium was placed on a dust basin.
2. Explosion vessel was cleaned including the electrodes and screwed/locked on the base followed by the connection of wiring through the electrodes as shown in Figure 3-1 and Figure 3-4.
3. A supply voltage is applied in the circuit and bypass resistor  $R_2$  was switched on, and switched off when the desired set voltage was attained which was monitored by a voltmeter.
4. Air blast and high speed camera is activated simultaneously.

5. When dust cloud reached the electrode gap, the electric spark discharged was triggered.
6. After each tests, supply voltage is turned off. And before disconnection of wiring, and detaching the explosion vessel, a voltmeter is monitored for unexpected charge remained in the circuit. Then explosion vessel is thoroughly cleaned. At high energy, the centre of hemispherical electrode is eroded. A fine sand paper was used to mend rough surface or changed the electrode.
7. After repeated tests, the condition of desired energy is reduced into half. The method continuous until no ignition reaction is observed. When no ignition reaction is observed, the energy is increased into half of the difference of the previous energy and existing value of energy used until MIE is attained, because of the difference of succeeding energy.

A limited number of experiments was performed on varied dispersion air pressure other than atmospheric pressure (3 bar and 3.5 bar) and twice the nominal stoichiometric concentration of lycopodium.

### 3.2.4 Measurement of discharge duration of spark discharges

The duration and behaviour in terms of decaying oscillation of the spark discharges was measured through oscilloscope instrument. The oscilloscope is triggered when a spark is discharged between the electrode gap. The spark discharge behaviour was visual analysis based on Figure 2-10. This is result is shown in Figure 3-6.

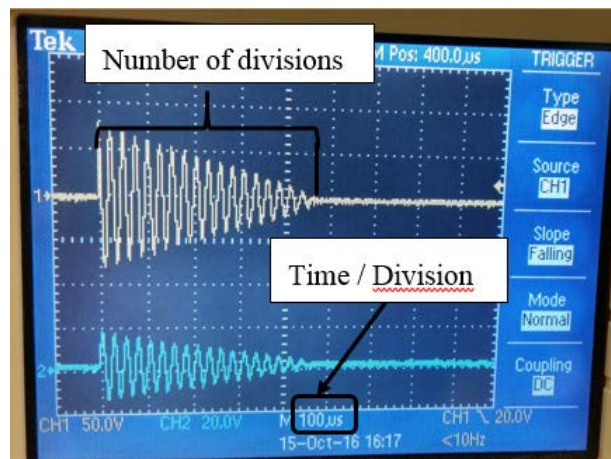


**Figure 3-6: Triggered spark discharge in oscilloscope display for measuring spark duration with an indication of important features.**

In Figure 3-6, the horizontal axis represents time that is divided into 10 divisions, equivalent to the number of squares. The time/division is also shown on the display.

Spark discharge duration is:

$$\text{Spark discharge duration} = \text{total no. of division} \times \text{time/division} \quad (3-1)$$

### 3.2.5 Estimation of spark energy

The basic method adopted was assumed that the spark energy was identical with the stored energy in the capacitor before spark discharge without any losses in the circuit. Another method of calculating the spark energy is by integrating the power versus time on the resulting oscillation as described by Olsen et al. (2015) and Randaberg et al.(2006b). But this is not adopted in the present thesis because of many oscillations that any possible error on each oscillation can affect the total value of spark energy.

However, another method was introduced in the present thesis. Spark energy is calculated by integrating half of the initial power with respect to time. The equation of initial power with respect to time is:

$$P_0(t) = \frac{1}{2} I^2 R \int_0^{\infty} e^{-\frac{Rt}{2L}} \quad (3-2)$$

Where  $P_0$  is the initial power in watt,  $I$  is the current in ampere and  $R$  is the resistance of spark in ohm.  $\int e^{-\frac{Rt}{2L}}$  represents the exponential decay in time that is calculated based on rule no.3 stated in Section 2.3 (Attenborough, 2003). Power with respect to time is equivalent to spark energy in the present thesis and expressed as:

$$E_S = P_0(t) = \frac{1}{2} I^2 R \left( \frac{L}{R} \right) \quad (3-3)$$

Resulting to:

$$E_S = P_0(t) = \frac{1}{2} LI^2 \quad (3-4)$$

The equivalent equation of spark energy is the same in equation 1-5. Therefore,

$$E_C = E_L = E_S \quad (3-5)$$

The stored energy in the capacitor is equivalent to the stored energy in the inductor.

$$\frac{1}{2} CV^2 = \frac{1}{2} LI^2 \quad (3-6)$$

### 3.2.6 Estimation of time constant, resistance and current of spark discharge

The equivalent circuit for the triggered electric spark discharges with or without additional inductance are shown in Figure 3-7.



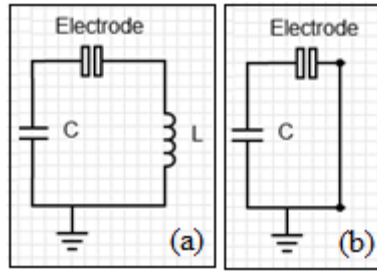


**Figure 3-7: Equivalent circuit for assessment of triggered electric spark discharge, (a) With additional inductor, (b) without additional inductor**

### 3.2.6.1 Time constant of spark discharge

Time constant is related to the total resistance in the circuit shown in Figure 3-7. The stored energy from the capacitor is consumed by the triggered electric spark discharged that shows exponential decay. The mathematical equation of exponential decay is:

$$y(t) = A e^{-\frac{t}{\tau}} \quad (3-2)$$

Variable  $y(t)$  is the amplitude (voltage or current) in a given time,  $A$  is the initial amplitude,  $t$  is time with negative sign that represents decay in second (positive sign means gain which is not the concern of the present thesis) and  $\tau$  is the time constant in second. Time constant is the time required for a voltage or current to rise and fall exponentially (Smith, 2002). From equation 3-2, when  $t = \tau$ , the initial amplitude decays to approximately 37% and the graphical representation is shown in Figure 3-8.

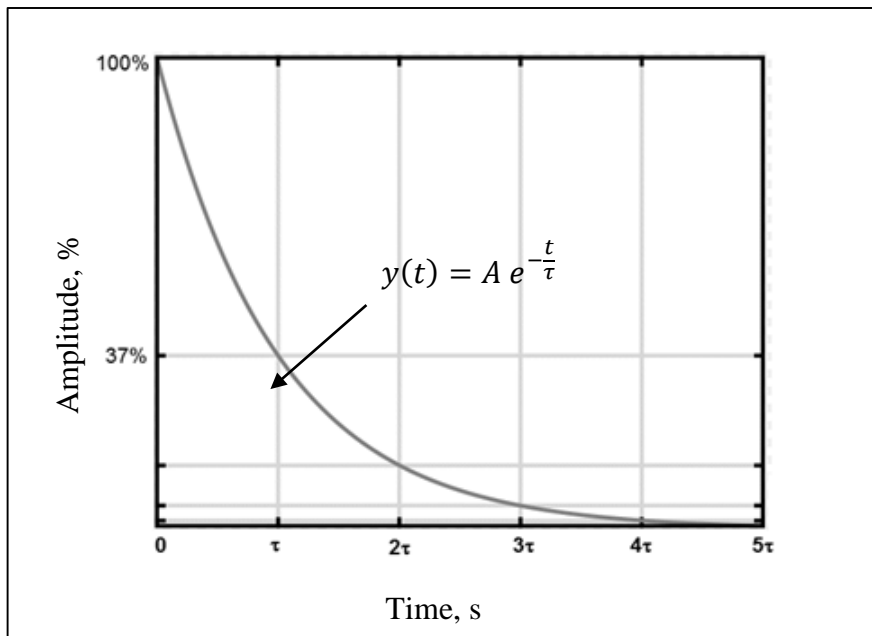


**Figure 3-8: Graphical representation of exponential decay of spark discharge current and voltage.**

From the measurement in oscilloscope, equation 3-2 is applied. The total number of period is counted and 37% of the total number of period is equivalent to time constant which is the same in Figure 3-8. Another equation of time constant is equation 2-2 to calculate the total resistance  $R_T$  in Figure 3-7.

### 3.2.6.2 Resistance

The gap between the electrode is equivalent to a resistor with resistance,  $R_S$ . Then the total resistance in the circuit shown in Figure 3-7 is:

$$R_T = R_S + R_L \quad (3-4)$$

where  $R_T$  is the total resistance in the circuit in ohm,  $R_S$  is the resistance of spark in ohm, and  $R_L$  is the resistance of inductor in ohm. The total resistance is calculated using equation 2-2 because  $R_S$  and  $R_L$  are unknown.

$R_L$  is calculated to evaluate the losses in the inductor using quality factor or known as Q-factor. The Q-factor determines the quality of the circuit in energy losses per period. A high Q-factor means that the ohmic energy dissipation is small, and a low Q-factor means that dissipation is large. Q-factor equation is:

$$Q = \frac{f_R}{BW} \quad (3-5)$$

Q is the quality factor that is dimensionless,  $f_R$  is the frequency response in hertz, and BW is the bandwidth in hertz.

First, Q-factor is calculated from the measured bandwidth in function generator and resonance frequency. Second, another equation of Q-factor to calculate the resistance of inductor is:

$$Q = \frac{1}{R_L} \sqrt{\frac{L}{C}} \quad (3-6)$$

$R_L$  is inductor resistance in ohm, L is inductance in henry, and C is capacitance in farad.

### 3.2.6.3 Current

Current is calculated from secondary oscillation that is out of phase shown on the display of oscilloscope which is the voltage across the resistor in the circuit stated in Section 3.2.1. Current is calculated using ohm's law:

$$I = \frac{V}{R} \quad (3-7)$$

Here, I is current in ampere, V is voltage in volt, and R is resistance in ohm.

All the collected data was manipulated in microsoft excel software. For simulation, cadence electronic design automation software is used in comparison with the actual measurement of oscilloscope.

## 4 Test dust

The dust used in the present investigation has been lycopodium clavatum. This dust is the spore of club moss, that grows in alpine, arctic regions and mainly in temperate zones. According to Kumar (2008), lycopodium is also called “trailing evergreens” and “ground pines”. The plant lycopodium clavatum is shown in Figure 4-1.

Mature lycopodium sporangium wither, and spores will rupture and a light yellow to orange colour lycopodium clavatum dust is released. The spores germinate in three to eight years. Only two of the many species of lycopodium dust are harvested, one of them is lycopodium clavatum (Thomas et al., 1991).

The morphology of lycopodium clavatum particle is verified and measured by means of scanning electron microscopy (SEM) shown in Figure 4-2.

The lycopodium clavatum particles are sculptured with reticulate ridges in tetrahedral outline and all have the same diameter of approximately 30  $\mu\text{m}$ . Based on Figure 4-2, it was concluded that the lycopodium dust used in the present investigation work was actually lycopodium clavatum. The chemical composition in mass % is 68.02% C, 19.88% O, 9.6% H, 1.32% N, 0.08% S, and 1.1% ash. The natural water content is 3.3–3.7% (Eckhoff, 1970).

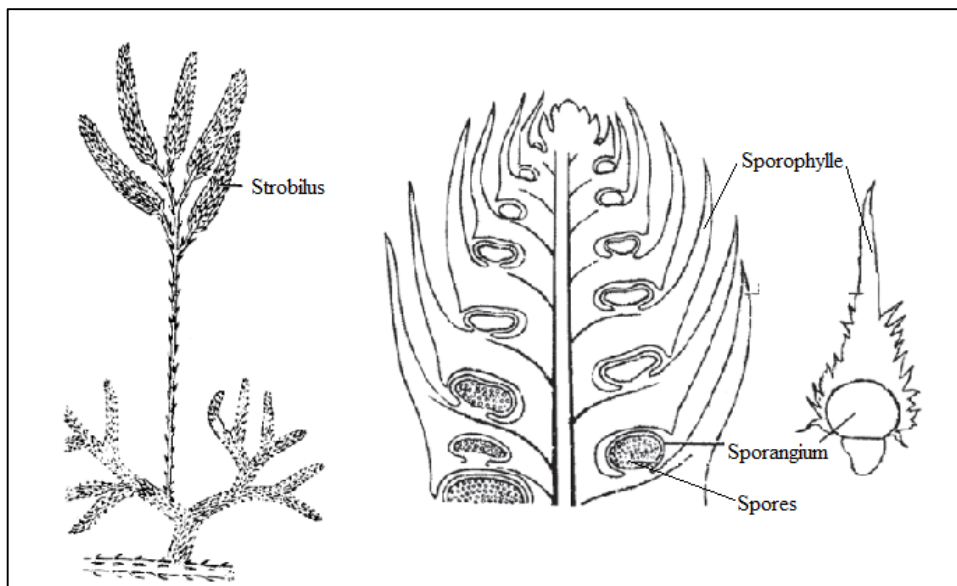


**Figure 4-1 Lycopodium clavatum. From Margaret (2008).**

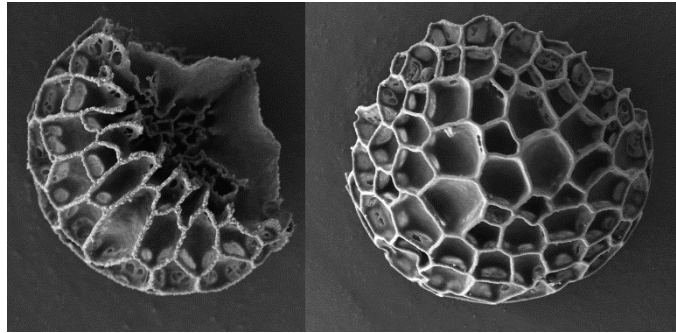


**Figure 4-2: SEM photographs produced by the University of Bergen electron microscopy laboratory.**

As reported by Eckhoff (2003) the density of lycopodium clavatum particles is  $1.18 \text{ g/cm}^3$  and the stoichiometric concentration is  $125 \text{ g/m}^3$ . For the explosion vessel used in the present experiment is 2.6 l, that the mass to be dispersed to achieve the stoichiometric concentration (nominal) is 0.3 g. Prior to the experiments with the lycopodium, the safety precautions to be taken were examined by reading the material safety data sheet of lycopodium dust (Sigma-Aldrich, 2014).

In addition to lycopodium, dust produced from manual rubbing of a piece of red coloured chalk was used in one specific experiment. Natural chalk is a soft, porous sedimentary carbonate rock (limestone). It is used in classrooms and manufactured by grinding natural chalk, adding water and clay as a binder, and rolled in a cylindrical dyer. Chalk dust sticks to surfaces easily, and is inert and non-toxic. Chalk dust was used in the present research for investigating a specific phenomenon during spark discharges using short discharge times.

## **5 Results**

### **5.1 Electric spark discharge decaying oscillation including the duration**

In all the experiments performed, the decaying oscillation of both voltage and current in time of the spark discharges (triggered by lycopodium dust clouds) were underdamped (damping response). This was the case of both with and without additional series inductor in the circuit, as well as for both electrode shapes (hemispherical and cylindrical flat-end).

Two examples of spark voltage versus time are shown in Figures 5-1 and 5-2. The two figures also show the respective durations of the two discharges. The stored capacitor energy was 256 mJ in both cases. The electrode shape was hemispherical in both cases, but an identical underdamped response is also produced with the cylindrical electrodes. The induced inductance of the circuit without additional series inductance was  $2 \mu\text{H}$ , and with added series inductance was 2 mH.

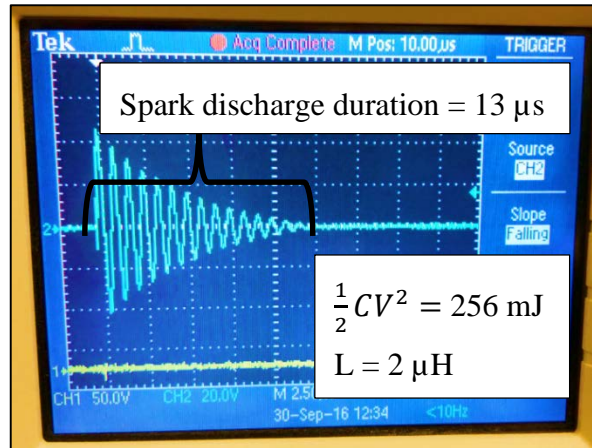


**Figure 5-1: Actual oscillation of spark discharge without additional series inductor in the circuit. Hemispherical electrodes.**

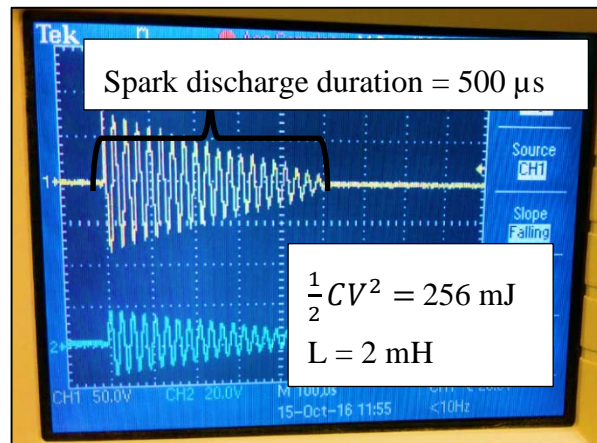


**Figure 5-2: Actual oscillation of spark discharge with additional series inductor in the circuit. Hemispherical electrodes.**

The measured mean spark discharge durations at atmospheric pressure, triggered by dispersing 0.3 g dust in the explosion vessel, are presented in Tables 5-1 and 5-2. The data in Table 5-1 was obtained with hemispherical electrodes of 10 mm diameter and the data in Table 5-2 was obtained with cylindrical flat-end electrodes of 1 mm diameter.

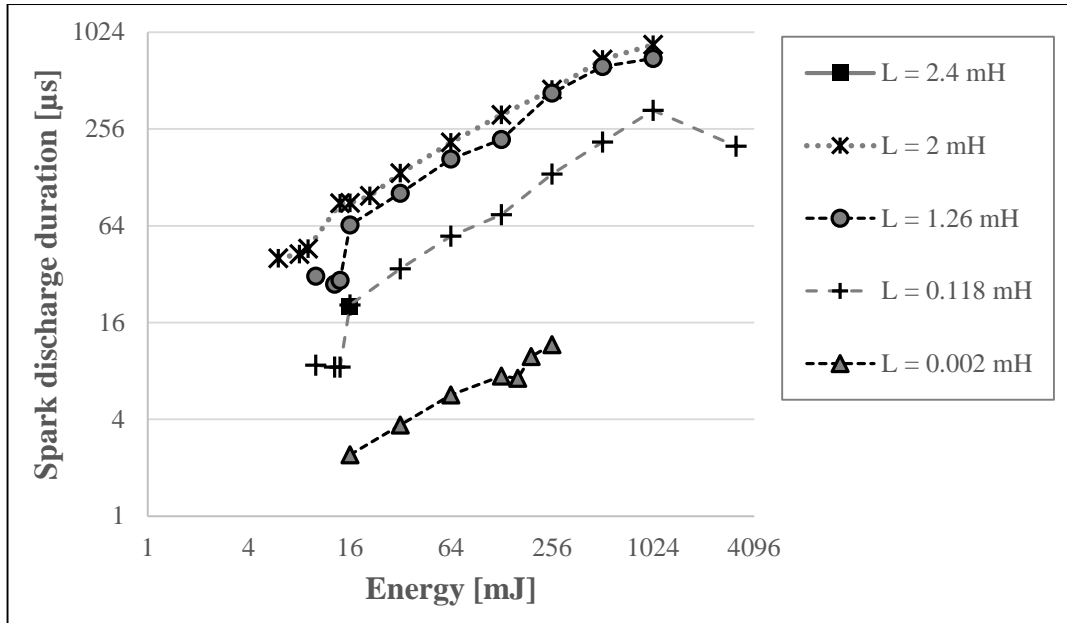
**Table 5-1: Mean electric spark discharge durations for discharges triggered by lycopodium dust cloud for hemispherical electrode of 10 mm diameter**

Mean spark discharge duration [ $\mu$ ]	Circuit inductance, $L$ [mH]					
	0.002	0.118	1.26	2	2.4	
Energy, $E_C$ [mJ]	6	-	-	-	$40 \pm 3$	-
	8	-	-	-	$43 \pm 4$	-
	9	-	-	-	$46 \pm 3$	-
	10	-	$9 \pm 1$	$31 \pm 5$	-	-
	13	-	$8 \pm 1$	$28 \pm 3$	-	-
	14	-	$8 \pm 1$	$29 \pm 4$	$88 \pm 18$	-
	16	2	21	65	$89 \pm 20$	20
	21	-	-	-	$98 \pm 16$	-
	32	4	$35 \pm 5$	$102 \pm 32$	$136 \pm 24$	-
	64	6	$55 \pm 5$	$167 \pm 5$	$211 \pm 45$	-
	128	$7 \pm 1$	75	$220 \pm 20$	$314 \pm 14$	-
	160	7	-	-	-	-
	192	$10 \pm 1$	-	-	-	-
	256	$12 \pm 1$	$135 \pm 8$	$429 \pm 44$	$451 \pm 73$	-
	512	-	$212 \pm 13$	$628 \pm 66$	$694 \pm 54$	-
	1024	-	$335 \pm 5$	$702 \pm 51$	$856 \pm 58$	-
3200	-	$200 \pm 5$	-	-	-	

**Table 5-2: Mean electric spark discharge durations for discharges triggered by lycopodium dust cloud for cylindrical flat-end electrode of 1 mm diameter.**

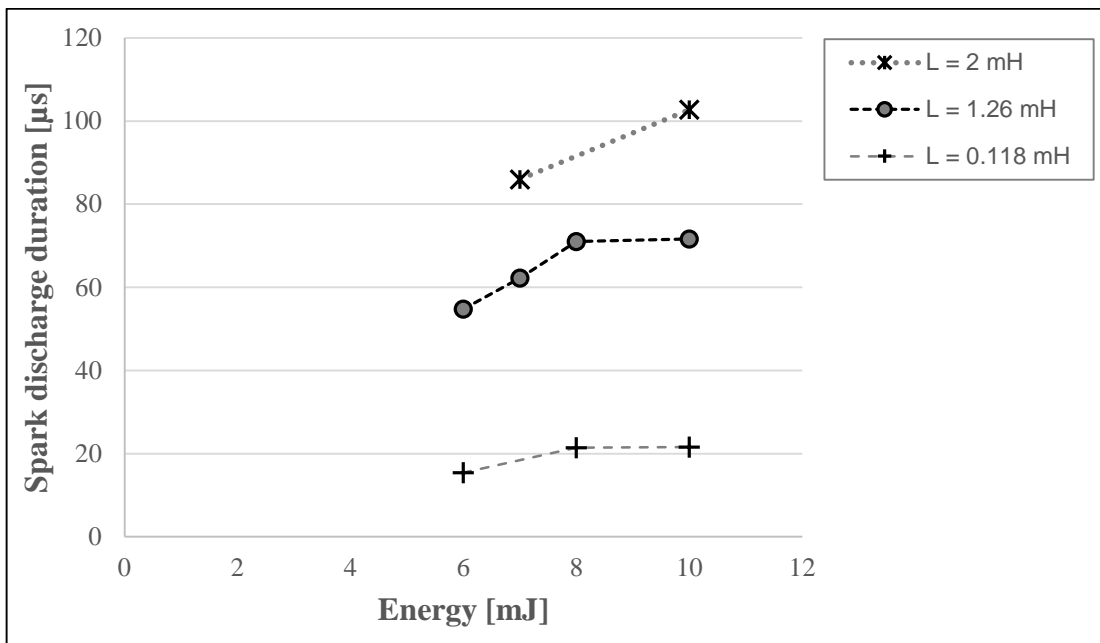
Mean spark discharge duration [ $\mu$ ]	Circuit inductance, $L$ [mH]			
	0.118	1.26	2	
Energy, $E_C$ [mJ]	6	$15 \pm 2$	$55 \pm 11$	-
	7	-	$62 \pm 9$	$86 \pm 10$
	8	$21 \pm 3$	$71 \pm 13$	-
	10	22	$72 \pm 14$	$103 \pm 24$

Figure 5-3 shows a graphical presentation of the data in Table 5-1 for hemispherical electrodes.



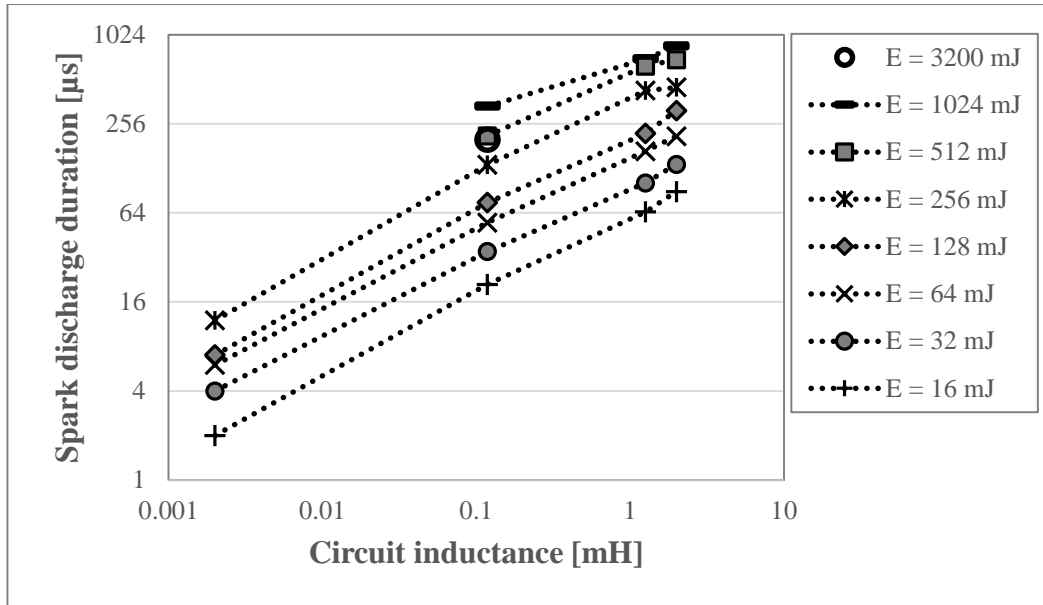
**Figure 5-3: Spark discharge duration as a function of spark energy. For hemispherical electrode.**

Figure 5-4 shows a graphical presentation of the data in Table 5-2 for cylindrical flat-end electrodes.



**Figure 5-4: Spark discharge duration as a function of spark energy. For cylindrical flat-end electrodes.**

The influence of inductance in the circuit on spark discharge duration is shown in Figures 5-5 and 5-6 for both electrode shapes.



**Figure 5-5: Spark discharge duration as a function of circuit inductance for hemispherical electrodes.**

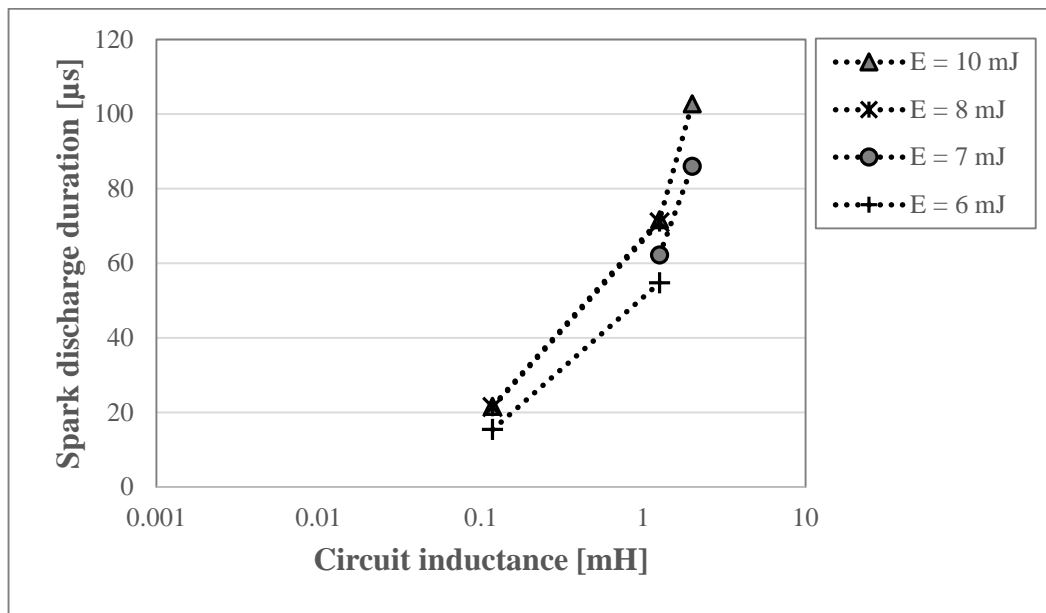


**Figure 5-6: Spark discharge duration as a function of circuit inductance for cylindrical flat-end electrodes.**

Other parameters were observed that influence the duration of spark discharges other than the stored energy and various inductances in the circuit.

### 5.1.1 Mass of dispersed dust

Spark discharge duration behaviour on different mass of dust dispersed in the explosion vessel at atmospheric pressure. This is illustrated in Figure 5-7.



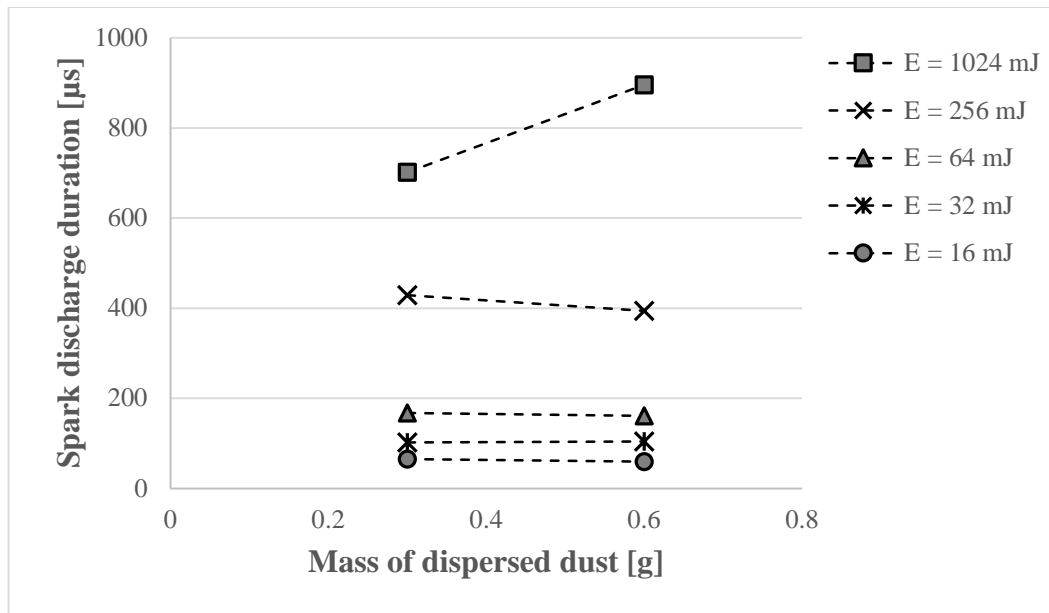


**Figure 5-7: Spark discharge duration as a function of mass of dispersed dust using hemispherical electrodes with an additional series inductance of 1.26 mH in the circuit.**

### 5.1.2 Dispersion air pressure

The spark discharge duration behaviour on different dispersion air pressure of the initiation of dust cloud for a given energy  $E_C$ . This is illustrated in Figure 5-8.

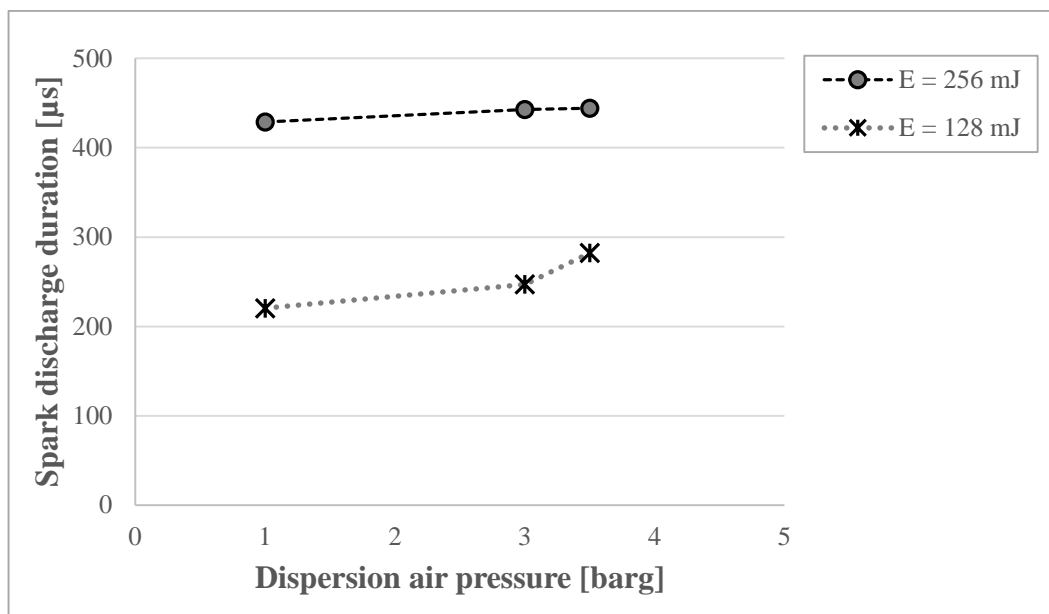


**Figure 5-8: Spark discharge duration as a function of dispersion air pressure using hemispherical electrodes with additional series inductance of 1.26 mH in the circuit.**

## 5.2 Estimated theoretical spark energies by two different methods

The two different methods were:

- Calculation of the equivalent stored energy  $E_C$  by the method described in Section 3.2.5 in Chapter 3.
- Calculation of the equivalent stored energy  $E_L$  by the method also described in Section 3.2.5 in Chapter 3.

In Tables 5-3 and 5-4 shows the estimated spark energies for hemispherical and cylindrical flat-end electrodes that illustrate the difference of spark energies  $E_L$  from various inductances. As can be seen, the results obtained by the two methods differs. The reason for this will be discussed in chapter 6.

**Table 5-3: Estimated spark energies by two different methods. Hemispherical electrodes.**

Stored energy, $E_C$ [mJ]	Mean energy measured, $E_L$ [mJ]	Inductance, $L$ [mH]	Mean energy measured, $E_L$ [mJ]
$\frac{1}{2}CV^2$	$\frac{1}{2}LI^2$		
8	8	2	8
9	9	2	9
12	12	2	12
33	33	0.118	34
		1.26	31
30	30	0.118	29
		1.26	30
31	31	0.118	50
		1.26	30
		2	14
18	18	0.002	12
		0.118	45
		1.26	23
		2	18
		2.4	19
23	23	2	23
49	49	0.002	33
		0.118	56
		1.26	33
		2	49
69	69	0.002	73
		0.118	75
		1.26	69
		2	67
144	144	0.002	133
		0.118	144
		1.26	133
		2	144
138	138	0.002	138
176	176	0.002	176
247	247	0.002	209
247	247	0.118	257
		1.26	250
		2	324
520	520	0.118	510
		1.26	530
		2	618
1087	1087	0.118	1028
		1.26	1226
		2	1278
3203	3203	0.118	3203

**Table 5-4: Estimated spark energies by two different methods. Cylindrical flat-end electrodes.**

Stored energy, $E_C$ [mJ]	Mean energy measured, $E_L$ [mJ]	Inductance, $L$ [mH]	Mean energy measured, $E_L$ [mJ]
$\frac{1}{2}CV^2$	$\frac{1}{2}LI^2$		
6	13	0.118	16
		1.26	10
7	9	1.26	8
		2	9
8	11	0.118	11
		1.26	10
10	13	0.118	17
		1.26	11
		2	12

### 5.3 Estimated time constants, resistances and currents of spark discharge

The estimated time constants, resistances and currents at atmospheric pressure, triggered by dispersing 0.3 g dust in the explosion vessel are presented in Tables 5.5 and 5-6 for both electrodes.

**Table 5-5: Estimated time constants, resistances and currents of spark discharge wave forms. Atmospheric pressure. 0.3 g of dust dispersed in the explosion chamber. Hemispherical electrodes.**

Energy, $E_C$ [mJ]	Inductance, $L$ [mH]	Time constant, $\tau$ [mH]	Resistance, $R_S$ [mH]	Current, $I$ [mH]
6	2	15	$264 \pm 18$	$3 \pm 0.22$
8	2	16	$250 \pm 22$	3
9	2	17	$230 \pm 16$	$4 \pm 0.5$
10	0.118	3	$112 \pm 8$	$24 \pm 5$
	1.26	12	$220 \pm 35$	7
13	0.118	3	$115 \pm 14$	$22 \pm 2$
	1.26	10	$246 \pm 35$	$7 \pm 0.32$
14	0.118	3	$115 \pm 12$	$29 \pm 5$
	1.26	11	$234 \pm 45$	$7 \pm 0.32$
	2	33	$123 \pm 30$	$4 \pm 0.34$
16	0.002	0.9	$4 \pm 0.42$	$110 \pm 3$
	0.118	8	$31 \pm 5$	$28 \pm 5$
	1.26	24	$107 \pm 24$	$6 \pm 0.82$
	2	33	$123 \pm 29$	$4 \pm 0.32$
	2.4	7	633	4
21	2	36	$109 \pm 19$	$5 \pm 0.44$
32	0.002	1	$3 \pm 0.27$	$182 \pm 3$
	0.118	13	$18 \pm 3$	$31 \pm 2$
	1.26	38	$68 \pm 17$	$7 \pm 1$
	2	50	$77 \pm 13$	$7 \pm 0.16$
64	0.002	2	$2 \pm 0.16$	$271 \pm 8$
	0.118	20	$11 \pm 2$	$36 \pm 1$
	1.26	62	$39 \pm 6$	$11 \pm 0.88$
	2	78	$49 \pm 11$	$8 \pm 0.61$
128	0.002	3	$1 \pm 0.08$	$365 \pm 21$
	0.118	28	$8 \pm 0.36$	$49 \pm 1$
	1.26	82	$28 \pm 3$	$15 \pm 0.86$
	2	116	$30 \pm 2$	12
160	0.002	3	$2 \pm 0.11$	$372 \pm 18$
192	0.002	4	$1 \pm 0.12$	$419 \pm 19$
256	0.002	4	$0.8 \pm 0.04$	$457 \pm 22$
	0.118	50	$7 \pm 0.5$	66
	1.26	160	$13 \pm 1$	20
	2	167	$20 \pm 3$	18
512	0.118	79	$3 \pm 0.2$	93
	1.26	234	$8 \pm 1$	29
	2	257	$12 \pm 1$	$25 \pm 1$
1024	0.118	125	$1 \pm 0.03$	132
	1.26	260	$7 \pm 0.7$	$44 \pm 0.7$
	2	317	$9 \pm 0.8$	$36 \pm 0.7$
3200	0.118	75	$3 \pm 0.1$	233

**Table 5-6: Estimated time constants, resistances and currents of spark discharge wave forms. Atmospheric pressure. 0.3 g of dust dispersed in the explosion chamber. Cylindrical flat-end electrodes.**

Energy, $E_C$ [mJ]	Inductance, $L$ [mH]	Time constant, $\tau$ [mH]	Resistance, $R_S$ [mH]	Current, $I$ [mH]
6	0.118	6	41 ± 5	16 ± 1
	1.26	20	123 ± 31	4
7	1.26	23	105 ± 19	4 ± 0.17
	2	32	117 ± 18	3
8	0.118	8	30 ± 4	13 ± 1
	1.26	26	93 ± 24	4 ± 0.24
10	0.118	8	29 ± 4	17
	1.26	27	92 ± 26	4 ± 0.17
	2	38	100 ± 28	3 ± 0.3

#### 5.4 MIE of lycopodium clavatum at nominal stoichiometric dust concentration

Different results of MIE  $E_C$  on varied inductances are summarized in Table 5-7.

**Table 5-7: Summary of MIEs of transient lycopodium dust cloud, ignited by triggered electric spark discharges of varying inductances**

Inductance, $L$ [mH]	Hemippherical electrodes		Cylindrical flat-end electrodes	
	MIE, $E_C$ [mJ]	Probability of ignition [%]	MIE, $E_C$ [mJ]	Probability of ignition [%]
0.002	192	3	Not tested	
0.118	16	5	10	5
1.26	16	8	7	8
2	14	20	10	3

The data stated in Table 5-7 was taken from the probability of ignition of the known energy on varied inductances in the circuit for both electrodes (hemispherical and cylindrical flat-end) at atmospheric pressure and 0.3 g of dust dispersed in the explosion vessel, illustrated in Figures 5-9 and 5-10.

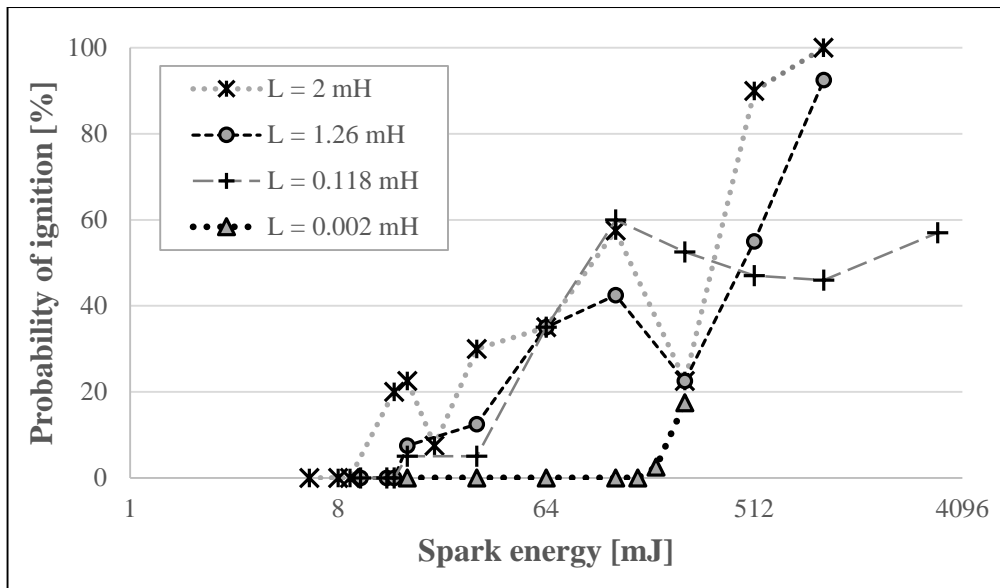


**Figure 5-9: Probability of ignition of transient lycopodium clavatum dust cloud as a function of spark energy in comparison to varying inductance for hemispherical electrodes.**

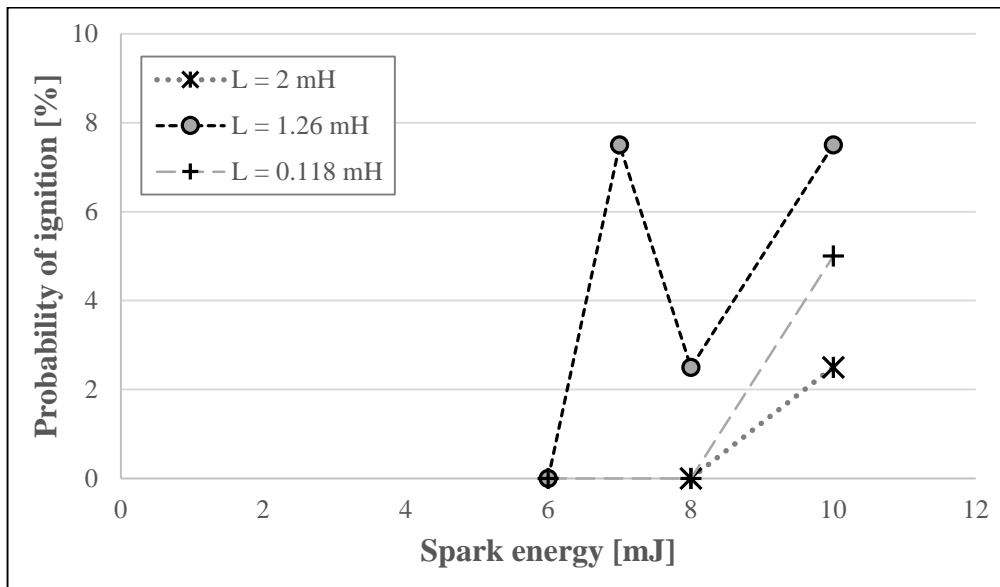


**Figure 5-10: Probability of ignition of transient lycopodium clavatum dust cloud as a function of spark energy in comparison to varying inductance for cylindrical flat-end electrodes.**

Based on Figure 5-9, the 20% probability of ignition on energy as a function of varied inductance in the circuit is illustrated in Figure 5-11.

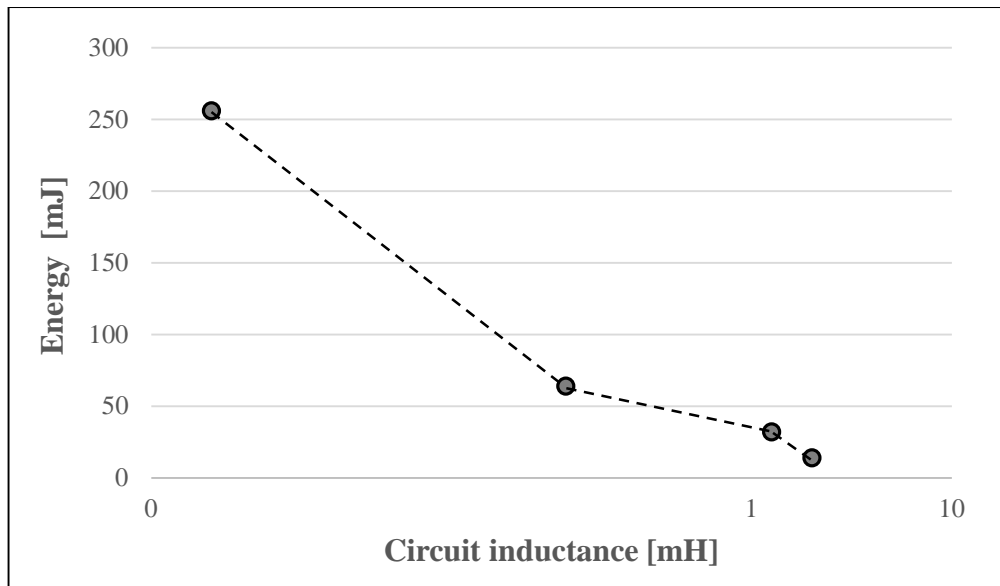


**Figure 5-11: Spark energy giving 20% probability of ignition as a function of varied inductance (with equivalent spark discharge time) in the circuit.**

## 5.5 Parameters that affects the ignition of lycopodium dust cloud

### 5.5.1 Dispersion air pressure

The influence of dispersion air pressure to the ignitability of the dust cloud were seen in the present thesis which are illustrated in Figures 5-12.

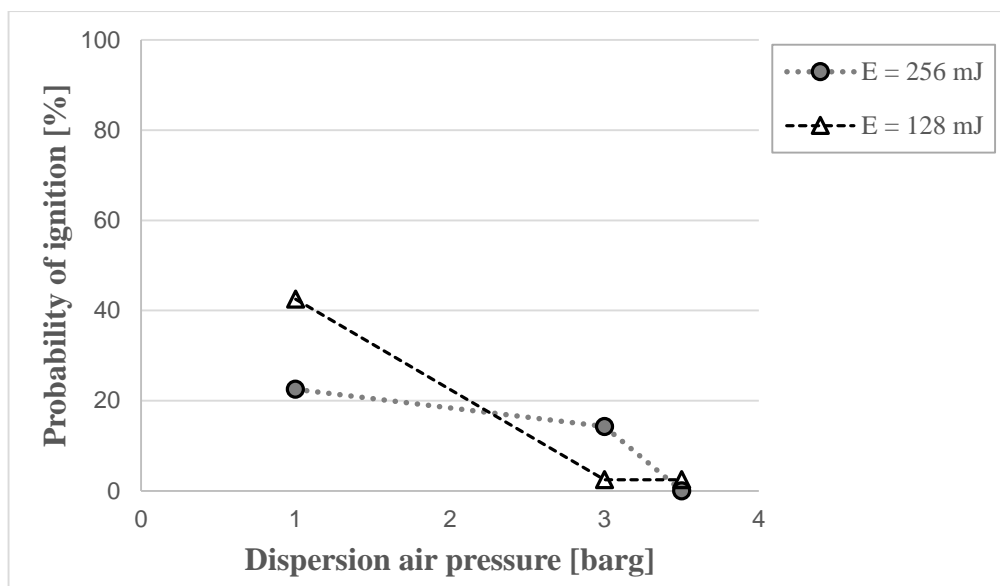


**Figure 5-12: Probability of ignition as a function of dispersion air pressure on a circuit with additional series inductance of 1.26 mH in the circuit for hemispherical electrode of a known energy and mass of dispersed lycopodium dust of 0.3 g in the explosion vessel.**



### 5.5.2 Concentration of lycopodium dust

The influence of dust concentration to the ignitability of the dust cloud were seen in the present thesis which are illustrated in Figures 5-13 for hemispherical electrodes of a given energy.

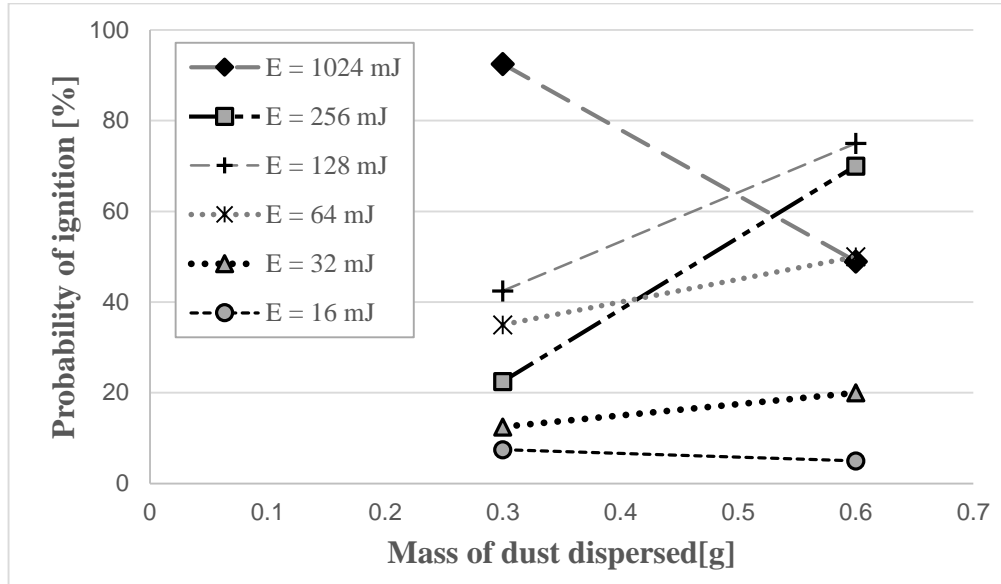


**Figure 5-13: Probability of ignition as function of mass of dust dispersed for hemispherical electrode in a circuit with additional series inductance of 1.26 mH.**

### 5.6 The relationship of spark resistance and energy

The gap between electrodes represent a resistor in the circuit. As lycopodium dust cloud is dispersed in explosion vessel, the resistance  $R_S$  changes as a function of energy  $E_C$  in reference to Section 5.4 and Tables 5-5 and 5-6. This is illustrated in Figures 5-14 and 5-15 on various inductances in the circuit for both type of electrodes used in the present thesis.

The spark resistance is also related to the third item on Section 5.9.

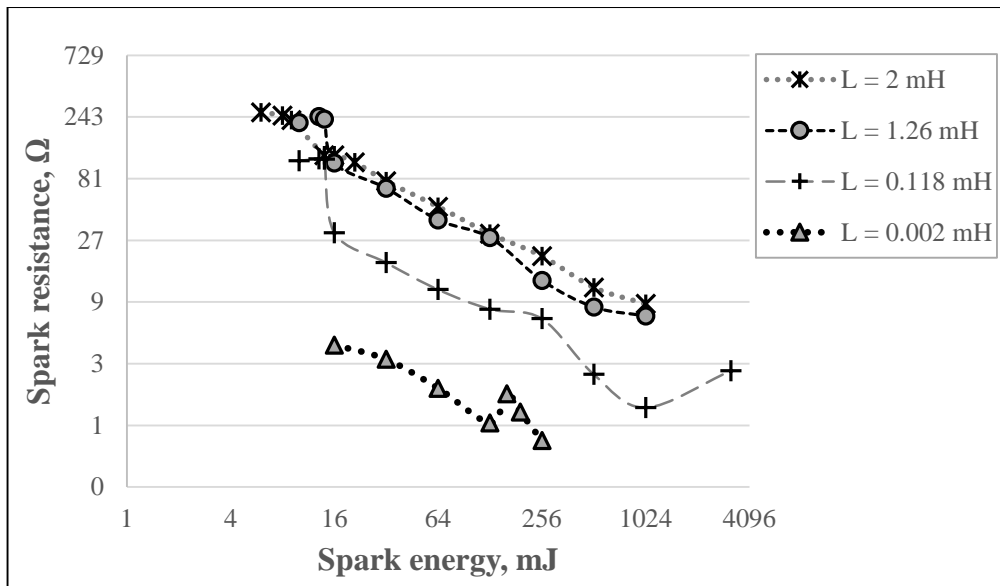


**Figure 5-14: Spark resistance as a function of spark energy for hemispherical electrodes.**

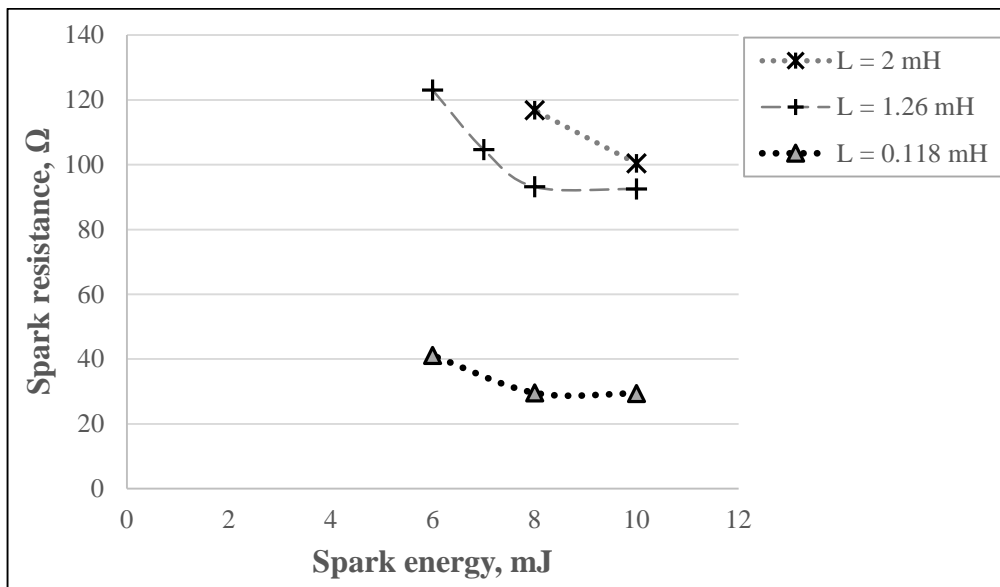


**Figure 5-15: Spark resistance as a function of spark energy for cylindrical flat-end electrodes.**

The effect of the actual spark resistance on the probability of ignition of lycopodium dust cloud with a given energy is illustrated in Figure 5-16.

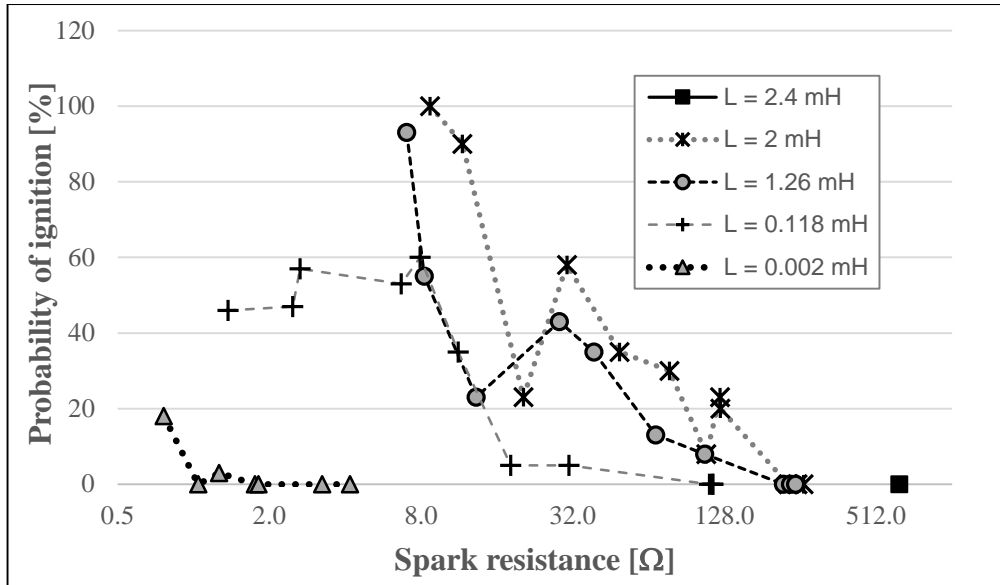


**Figure 5-16: Probability of ignition as a function of spark resistance**

### 5.7 Actual breakdown voltage in air and the set supply voltage difference

The actual breakdown voltage in comparison to Section 3.2.1 on the set supply voltage in relation to relative air humidity are illustrated in Figure 5-17.

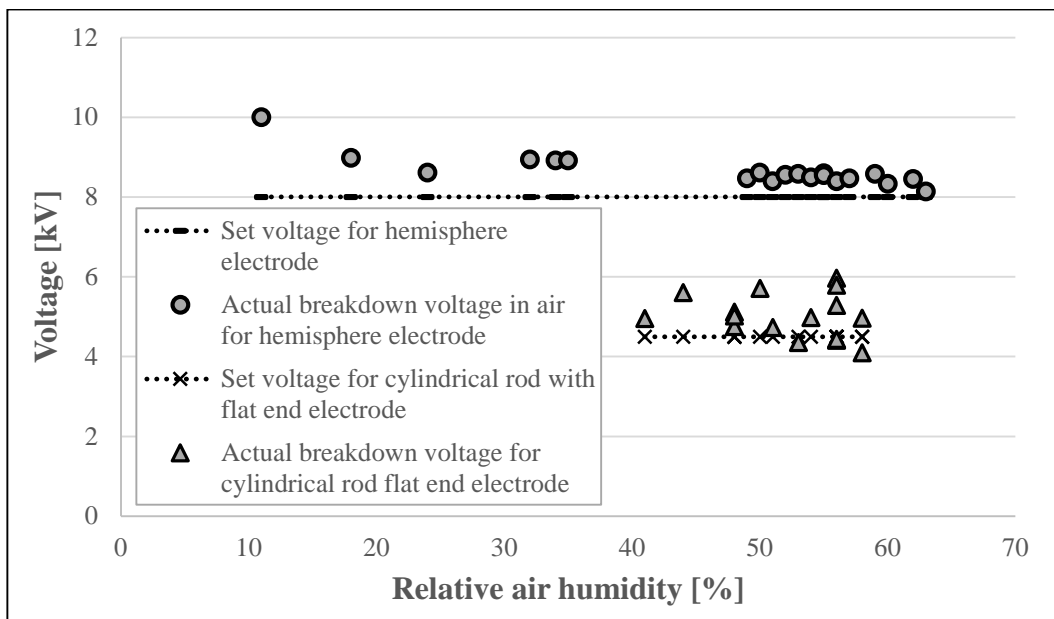


**Figure 5-17: Influence of humidity to actual breakdown voltage in air including the difference to the set supply voltage for both types of electrodes.**

### 5.8 Simulation of spark current and voltage as a function of time

A mathematical simulation of current and voltage development during an underdamped spark discharge of the same type as shown in Figures 5-1 and 5-2 was

performed using the Cadence software. Details of the software were not explored in the present study. The result of the simulation is shown in Figure 5.18. As can be seen, the pattern is very similar to the patterns in Figure 5-1 and 5-2.

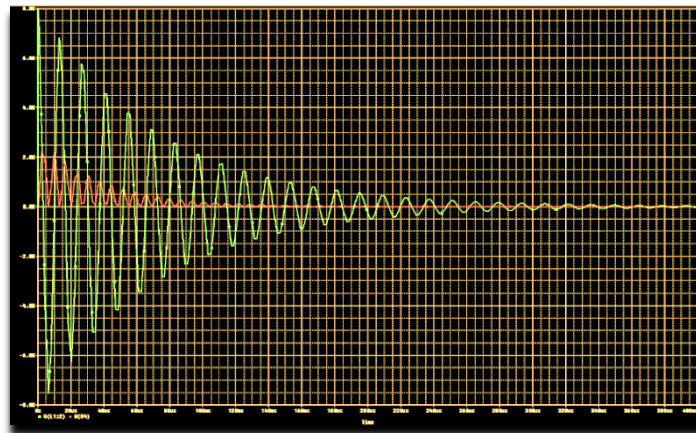


**Figure 5-18: Simulation of electric spark discharge current and voltage in a circuit with additional series inductance of the order of 2 mH. Full horizontal scale about 500  $\mu$ s.**

### 5.9 Additional phenomenon observed.

1. In 3470 experiments, approximately 10% of all the experiments performed in the present study, breakdown of the spark gap did not occur after the dispersion of the 0.3 g of lycopodium clavatum in the explosion vessel.
2. It was observed that, as soon as high voltage had been applied to the electrode gap, and prior to dust dispersion by the air blast, particles from the heap of lycopodium in the dispersion cup tended to be lifted-off the heap and migrate upwards and outwards to the internal surface of the explosion vessel that triggered the spark discharge. This effects appeared to be more pronounced with the cylindrical flat-end electrodes than with the hemispherical electrodes.
3. The luminous ball observed by high speed camera during spark discharges by the actual breakdown voltage in air was bigger in the circuit without additional inductor than the luminous ball created in the circuit with additional inductor. This is illustrated in Figure 5-19. The spark resistance without additional inductance in the circuit is low.

However, in Figure 5-20 shows a strange phenomenon as detected by the high speed camera. The luminous ball is more pronounced when spark discharge is triggered by dust cloud. In both cases (without and with additional series inductance) the figures shown three frames separated by about 0.3 ms. For both cases the first frame shows just a thin spark channel (not readily seen in the photographs). The second frame in both cases shows the maximum size of an illuminated “ball”, the nature of which has not been disclosed. It was definitely not a burning dust cloud, because when the vessel was cleaned after a test, there was no smoke or smell of smoke, and no carbonized dust, only fully unburnt dust.

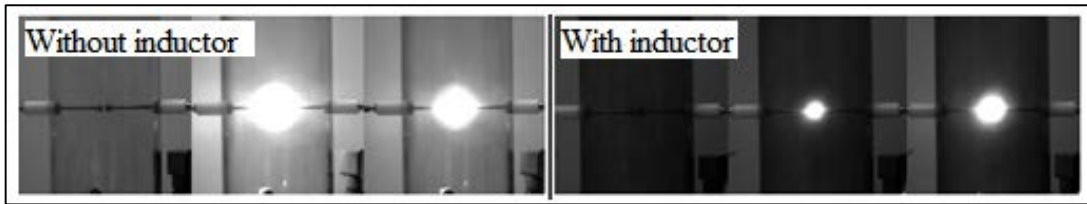


**Figure 5-19: Electric spark discharge in air without dust-particle triggering. 10 mm hemispherical electrodes. “Without inductor” means only inherent circuit inductance of 2  $\mu$ H. “With inductor” means an added series inductance of 2 mH.**

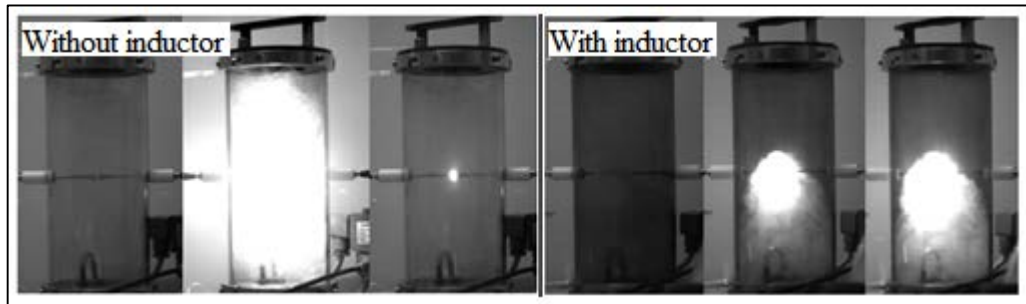


**Figure 5-20: Electric spark discharged triggered by transient lycopodium dust cloud.**

4. Figure 5-21 shows an example of “flamelet” captured by high-speed camera just after a spark discharge triggered by dust.

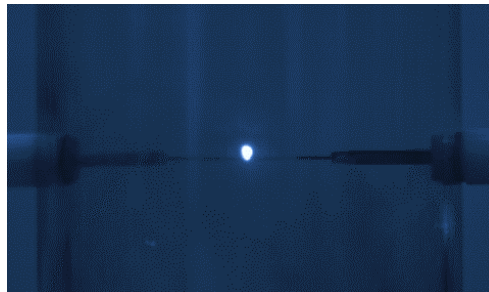


**Figure 5-21: Captured flamelet after electric spark discharge is triggered by transient lycopodium clavatum dust cloud.**

The flamelet extinguished less than 10 ms after the electric spark had been discharged. In the case shown, with an added 2 mH inductance in the circuit the electrodes were of the cylindrical flat-end type. However, the same phenomenon was also observed with the 10 mm diameter hemispherical electrodes on additional series inductances in the range 0.1 to 2 mH in the discharge circuit. The photographs of the complete build-up of a flamelet are shown in Appendix B.

5. In the experiments where the hemispherical electrodes had been covered by powdered red chalk prior to a spark discharge, the chalk layer was blown away by a 256 mJ spark from an electric circuit without additional inductance (hence only the inherent inductance of 2  $\mu$ H in the circuit). The result is shown in

Figure 5-22. As can be seen there is a dust free circular area of approximately 6 mm in diameter on both electrodes. With an additional series inductance of about 2 mH in the circuit, the 256 mJ spark discharge did not blow away any visible part of the dust on the electrodes. The likely reason for this is discussed in Chapter 6.

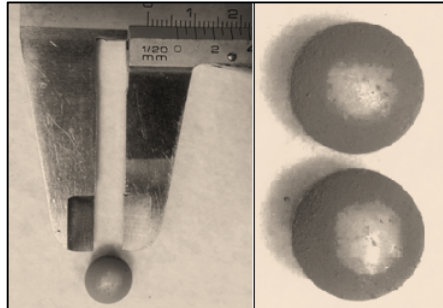


**Figure 5-22: The 10 mm diameter hemispherical electrodes with the dust free areas after a 256 mJ electric spark discharge from a circuit with just 2  $\mu$ H inherent inductance (no additional series inductance).**

6. The high speed camera also disclosed that the time of lycopodium dust cloud dispersion from dust basin to the appearance of the front of the lycopodium dust cloud at the spark gap was approximately 40-43 ms (dust dispersed was 0.3 g and 1 bar dispersion air pressure).  
From the front of dust cloud and spark gap, the spark discharge was not triggered instantly. There was a delay of spark discharge. This delay increased markedly with decreasing spark energy. Hence, with a spark energy of the order of 10 mJ the delay was  $> 1$  s, whereas it was only  $< 3$  ms with approximately 1 J spark energy. It was also observed that, with a given spark energy, the probability of ignition, increased with increasing delay between the moment of dust cloud front appearance at the electrodes, and moment of spark discharge.

## 6 Discussion

### 6.1 Practical industrial scenario for which the present investigation is relevant

Consider a metal silo that has by accident been left unearthed, as illustrated in Figure 1-12 in Chapter 1. The silo is loaded with a dust that has been charged electrostatically by previous tribo-electric processes in the plant. The loading causes electrostatic charging of the silo body either by charge influence and/or by charge diffusion from the powder to the silo (depending on the electrical conductivity of the dust). If the silo is loaded with the charged powder over some time, the voltage of the silo body with respect to ground will also raise gradually. Eventually a voltage may be reached at which a spark discharge can occur across some small gap between the silo body and ground. However, at this moment there may not be any explosible dust cloud in the region of the spark discharge, and no dust explosion will occur.

The present investigation focuses on the fact that a spark discharge can in fact occur in a situation that a transient dust cloud can accidentally enter a potential spark

gap before the gap voltage has reached the level of breakdown voltage. In such a case the process itself provides the synchronization between appearance of a dust cloud and the spark discharge that is needed for an accidental dust explosion to occur.

## 6.2 Electric spark discharge decaying oscillation including the duration

All electric spark discharge decaying oscillation of electric spark discharge in time are underdamped. Because even without additional inductor in the circuit, the cables itself induce magnetic flux in a flat wire, and the calculated inductance of the cable is approximately 2  $\mu\text{H}$  which are shown in Figures 5-1 and 5-2 in Section 5.1.

The energy presented in the shown figures above is the stored energy in the capacitor  $E_C$  which is equivalent to spark energy as discussed in Section 3.2.5. The spark discharge duration depends on the energy stored in the capacitor which are illustrated in Figures 5-3 and 5-4. As the energy increases the spark discharge duration increases that only varies with different inductance in the circuit. However, the actual spark discharge duration differs on repeated tests and that the data presented are the arithmetic mean including the standard deviation.

In Figure 5-5, an energy of 3 J was expected to be a longer spark discharge duration compare to 1 J but a gradual drop of spark discharge duration was encountered with series inductance of 0.118 mH, because of possible saturation in the circuit. The experiment at 3 J was then limited to 0.118 mH only because of the encountered saturation.

Another encountered drop of spark discharge in Figure 5-5 is at 16 mJ with inductance of 2.4 mH. The inductors used in this circuit was an improvised inductor of a wire coiled in two U-shaped ferrite magnet connected together forming an O-shaped to increase inductance to 2.4 mH, without realizing the limitation of ferrite magnet that exceeded to saturation point of 5 tesla resulting to shorter electric spark duration with few oscillations. The U-shaped ferrite magnet has a limited magnetic flux to about 0.35 tesla. Therefore, 2.4 mH was excluded on the succeeding experiments.

To avoid saturation on improvised inductor, a wire coiled in U-shaped ferrite magnet is maintained and two additional inductors are created on a separate U-shaped ferrite magnet connected together in series to increase the inductance producing a total inductance of 2 mH. However, this is the maximum inductance created due to the availability of U-shaped ferrite magnet.

Another observation were a lycopodium dust concentration and dispersion air pressure have no significant influenced on spark discharge duration which are shown in Figures 5-7 and 5-8 in Section 5.1. However, at high energy a significant increase of spark discharge duration was observed on a 0.6 g dust dispersed in the explosion vessel.

## 6.3 Spark energies

The derived equation of spark energy in Section 3.2.5 resulted to the energy stored in the capacitor  $E_C$  is equivalent to the energy stored in the inductor  $E_L$ . However, in Table 5-3 and 5-4 the equivalent energies of the experiments are different. The energy  $E_L$  also varies with the inductance because of the effect of the measured current.

Equation 3-6 is an ideal condition. The possible reason of discrepancy of spark energies between  $E_C$  and  $E_L$  are due to a low accuracy of actual current measured in the circuit. The simplest method of measuring the current is through series low resistance as discussed in Section 3.1.4. However, an induced inductance within the resistor itself is possible resulting to either slightly increase of energy in  $E_L$  compare to  $E_C$ . A complex method to calibrate the resistor for measuring the current was not applied in the present thesis. Another reason was a possible loose connection within the soldered components, a possible capacitor defect or some losses in the inductance itself and the influence of dust cloud either electrons are absorbed or gain.

#### **6.4 Time constant, resistance and current**

The time constant  $\tau$  is proportional to the spark discharge duration that are discussed in Section 6.1. The measured current  $I$  of a given energy is related to the calculated energy  $E_L$ . In Section 6.2 discussed the measured current in detail.

Spark resistance  $R_S$  is presented because it defines the following:

- The luminous ball of electric spark discharge which are shown in Figures 5-19 and 5-20 were observed that at low spark resistance produced a big luminous ball/intense glow like a welding arc and high current for the circuit without series inductor and vice versa with additional series inductance in the circuit. This is why the experiment performed without inductor in the circuit is limited to 256 mJ only which has a current of 457 A that are shown in Table 5-5. With high amount of current, the electrodes are prone to erosion and if the experiment performed is greater than 256 mJ, the electrodes will melt including the insulation of wires. This luminous ball or intense glow phenomenon observed in the present thesis corresponds to the report of Randeberg (2006).
- The contact between lycopodium dust cloud and the surface of electrodes. In Figure 5-14, 5-15 and 5-16 illustrates the effect of spark resistance on probability of ignition on various inductances. The spark resistance on the larger inductance is greater than the smaller inductance. This also indicates the greater contact of dust to electrodes.

#### **6.5 Minimum ignition energy**

In Figures 5-9 and 5-10, the probability of ignition to increasing energy is not linear because of the influence of humidity and turbulence. But when the energy is 1 J that is the longest duration of spark, the influence of humidity and turbulence and other possible factors are neglected as 100% of ignition was established in hemispherical electrodes. The experiments performed for cylindrical flat-end electrodes are limited for circuit with series inductance and with low energy to concentrate directly on the determination of MIE of lycopodium dust cloud. And because of the unstable characteristic and sensitivity of the electrodes that electric spark is discharged early (before dust cloud is released and if dust cloud is released, electric spark is discharged before electrodes are reached). The unstable characteristic of cylindrical flat-end electrode is also shown in Figure 5-10.



Another factor that influence the probability of ignition on a circuit without inductor in the circuit is due to shock wave, dust cloud is blown away that corresponds to Eckhoff (1970). The low probability of ignition are shown in Figures 5-9 and 5-10.

Different MIE results shown in Figure 2-7 of different electrode shapes was obtained by triggered electric spark by dust cloud that is limited only in nominal stoichiometric concentration of lycopodium dust cloud. However, the obtained MIE results are within the range of MIE of lycopodium based on BIA (1997).

For hemispherical electrodes the MIE is 14 mJ with electric spark duration of 88  $\mu$ s, and for cylindrical flat-end electrodes the lowest MIE is 7 mJ with electric spark duration of 62  $\mu$ s. The desired electric spark duration is longer than the presented results in the present thesis for low energy, but with big inductance in the circuit and high-frequency exceeds to saturation limit.

Several experiments are conducted on various dispersion air pressure other than atmospheric pressure. In Figures 5-12 and 5-13, the probability of ignition is decreasing on increasing pressure for a given energy. A dispersing air pressure of 3.5 bar of 256 mJ, no ignition occurred as illustrated in Figure 5-12. This is the effect of turbulence in accordance to Eckhoff (2003).

Regardless of varied inductance, the effect of ignition on two various concentration of dust were increasing as the concentration increases as illustrated in Figure 5-13. However, a sudden drop of probability of ignition in highest energy (1 J) used in twice the nominal stoichiometric concentration of lycopodium dust. The possible reason for this phenomena was the released heat or energy is too much that dissipates fast at greater concentration than lesser concentration. The lycopodium dust acts like a heat sink resulting to a sudden drop of probability of ignition.

## **6.6 Difference between set supply voltage and actual breakdown voltage**

About 3470 experiments are performed and triggered electric spark discharged from transient lycopodium clavatum dust cloud was obtained that corresponds to the report of Eckhoff and Randaberg (2006), but approximately 10% of the total number of experiments performed did not trigger the electric spark. The possible reasons are the following:

1. The influence of “high” humidity.

Both types of electrodes set supply voltage in the present thesis is 5% less than the mean actual breakdown voltage in air, and the experimental set up is based on practical situation in industry that humidity is not controlled. When the humidity is high, the difference between the actual breakdown voltage and the set voltage is small but electric spark discharge is not triggered by transient lycopodium dust cloud. Because of high moisture content on dust, but lycopodium clavatum dust resist water. The possibility of lycopodium dust to absorb moisture would take some time. An additional experiment is performed; a 5 g of lycopodium dust was placed in a closed cylinder with half-filled water for three months. After three months, lycopodium dust was not soaked in water, lycopodium is floating even if the hand was dunked through the water, the hand was shielded by lycopodium. After 3 months, lycopodium

dust coagulated forming a layer of cake. Therefore, the sensitivity of lycopodium dust in moisture is low.

At this point, lycopodium clavatum dust cloud may not be conductive enough to create a path between the spark gap, because the loss of tribo-electric charge is greater than the accumulated tribo-electric charge of lycopodium dust cloud. When lycopodium cloud was generated, it is also charged known as tribo-electric charge because of the friction on the wall of explosion vessel and lycopodium dust cloud. And according to Radwan et al. (2000) water in air helps the electrons to leak quickly and before lycopodium dust cloud reached the electrode, it is no longer conductive and no path is created.

2. The big difference between the actual breakdown voltage in air and set voltage at “low” humidity, at approximately 20% difference as illustrated in Figure 5-17. Considering the difference is big, that the accumulated energy is not sufficient to trigger the spark discharge. However, at low humidity the accumulation of electrostatic charge is high that the electric spark discharge is still possible which is established in the performed experiment.

The influence of low humidity on increasing actual breakdown voltage in air and high humidity on decreasing actual breakdown voltage in air that established in the present thesis corresponds to the statement of Salam et al. (2000).

## **6.7 Delay of electric spark discharge and captured flamelet**

There was a delay of electric spark discharge triggered by transient lycopodium dust cloud. From the point of contact between dust cloud to electrodes to trigger electric spark discharge has an “activation time”. The activation time is not constant. A longer activation time was observed on decreasing energy and vice versa as stated in Section 5.9. On a specific energy, the longer activation time induce ignition resulting to dust explosion than with shorter activation time induced electric spark discharged only on the circuit without inductor. The circuit with additional series inductor of shorter activation time established a flamelet that extinguished fast ( $< 10$  ms) that human eye cannot capture such phenomena. Longer activation time has greater concentration of dust cloud than in shorter activation time of spark discharge.

The settling time of lycopodium dust cloud was also verified compared to the activation time observed in the present thesis. Activation time is less than the time of dust cloud to settle in the gravitational field which is approximately 8 seconds based from Stokes and 16 seconds based from Eckhoff (1970) (Settling velocity of lycopodium dust cloud from Stokes is 0.035 m/s and from Eckhoff is 0.017 m/s).

Captured flamelet shown in Figure 5-21 could be a form of *cold* flame. A cold flame was discovered by Sir Humphry Davy in 1890. An ignition source such as spark was unnecessary to attain ignition because of certain limits like temperature (Chapek and Neville, 2016). The temperature of cold flame that encountered in experiments are not measured but the recorded cold flame temperature is less than 400°C (Wikipedia.org, 2016) and from Eckhoff (2003), minimum ignition temperature (MIT) of lycopodium clavatum is 460°C. If the flamelet captured is the same as a cold flame with a temperature range less than MIT of lycopodium clavatum,

then this might be the possible reason that ignition from flamelet in the present thesis is not established. However, this phenomenon is not been found in combustible dust.

## **6.8 The influence of electrostatic charge on the wall of the explosion vessel**

The explosion vessel was made from an electrically non-conducting transparent plastic tube. The observations made in the present work indicates that this tube may have given rise to unwanted electrostatic effects during experiments. There was indications that low humidity enhanced the electrostatic charging of the wall of explosion vessel. It was observed that dust particles in the dispersion cup at the vessel bottom migrated upwards in the explosion vessel and were attracted towards the charged wall of explosion vessel. This particle migration was the unintended triggering of the electric spark discharge during charging. It appeared that this tendency was more pronounced with the cylindrical flat-end electrodes than with the hemispherical electrodes.

# **7 Conclusions and suggestions for further work**

## **7.1 Conclusions**

1. In the present investigation synchronization of the appearance of the dust cloud at the spark gap and the spark discharge was obtained by first pre-charging the gap to a voltage lower than the natural breakdown voltage in air. The breakdown then occurred very shortly after the dust particles had entered the spark gap. It was observed by high-speed camera that with a given spark energy and discharge time, ignition did not occur if the delay between the first appearance of dust particles at the spark gap and spark discharge was less than a few milliseconds. If this delay of spark discharged was at least 10 ms, ignition occurred more frequently. It is suggested that this was because with short delays, only the low-concentration front of the dust cloud obtained a contact with the spark, whereas with longer delays, the spark discharge occurred in dust clouds of higher dust concentrations that were more readily ignitable.
2. The maximum diameter of the luminous spark kernel, as observed by high-speed camera at about 0.3 ms after onset of spark discharge, was considerably larger for spark durations of about 10  $\mu$ s than for durations of about 500  $\mu$ s.
3. In some cases, the spark discharge only generated a flamelet adjacent to the spark gap. Normally such a flamelet would extinguish within 10 ms. However, sometimes it appeared from the high speed camera that it moved around throughout the explosion vessel before extinguishing. An explanation of this phenomenon has not yet been found.
4. The influence of the mass of dust dispersed on the spark discharge duration was investigated for a range of spark energies, but no significant influence was found.
5. The influence of the dispersion air pressure on spark discharge duration was investigated for a range of spark energies, but no significant influence was found.

6. It was found, using two different electrode geometries (10 mm diameter hemispherical electrodes and 1 mm diameter cylindrical flat-end electrodes), had a significant influence on the ease by which the spark gap was breaking down at a given pre-set spark voltage, both in air only and when being broken down by dust particles. This is in accordance with expectations.
7. It was also found that dust-particle-triggered 0.3 J electric spark discharges with only 2  $\mu\text{H}$  inductance in the discharge circuit (short discharge time) produced a strong blast wave that would blow the dust cloud away from the spark region and hence lessen the probability of ignition. This is in agreement with the work by Line et al. (1959), and Eckhoff and Enstad (1976).
8. The present investigation has confirmed, when using electric sparks of discharge times of the order of 1 ms, that MIEs of clouds of lycopodium clavatum in ambient air is of the order of maximum 10 mJ, also when using the spark triggering method adopted in the present work. However, this was obtained with an added series inductance of 2 mH in the discharge circuit. The question is then whether series inductances of this magnitude can occur during accidental electrostatic spark discharges in industrial plant. It may appear that in industry that it is more likely prolonged spark discharge duration can be brought about by some kind of series resistance in the discharge circuit, e.g. a corroded ground connection. In that case, 90% or more of the stored capacitor energy will be dissipated in the series resistance, and on 10% or less in the spark. This would mean that the minimum stored energy in the capacitor that could cause ignition of clouds of lycopodium clavatum in ambient air would be 100 mJ or more, rather than 10 mJ or less.

## 7.2 Suggestion for further work

1. Further experimental studies of effects of various parameters on MIE, e.g.:
  - Quantity of lycopodium dispersed.
  - Other dusts (natural organic, plastics, metals).
  - Dispersion air pressure.
  - Sizes and shapes of electrodes (see possible versions in Figure 7.1).
  - Electrode materials.
  - Spark gap distance.
  - Effect of the difference of actual pre-set spark gap voltage and natural breakdown voltage in air only, on MIE.
  - Effect of increased series inductance  $> 2$  mH in the discharge circuit.
  - For future experiments it may be advisable to replace the plastic explosion vessel by one made of an electrically conducting and earthed metal one.



**Figure 7-1: Electrodes: (a) Circular with flat-end (10 mm  $\varnothing$ ), (b) Pointed (10 mm  $\varnothing$ , 45°), (c) Pointed (6.5 mm  $\varnothing$ , 20°).**

2. More fundamental issues related to the spark gap breakdown mechanism:
  - What is the influence, if any, of particle type, particle concentration and particle velocity on breakdown efficiency?
  - What is the influence, if any, of electrode material on breakdown efficiency?
  - What is the influence, if any, of electrode shape on breakdown efficiency? (consider also non-symmetrical electrode pairs of different shapes and metals)
  - What is the influence, if any, of the difference of actual pre-set spark gap voltage and natural breakdown voltage in air only, on MIE.

## References

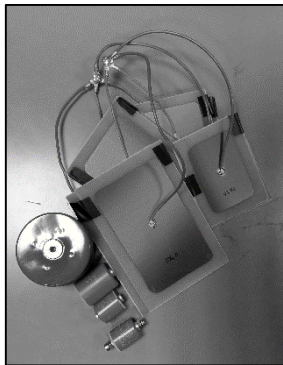
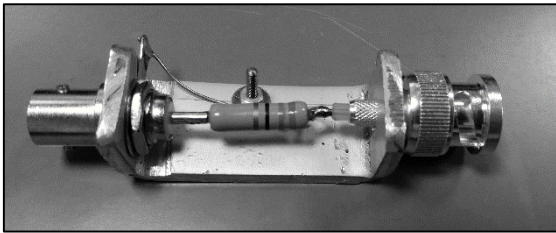
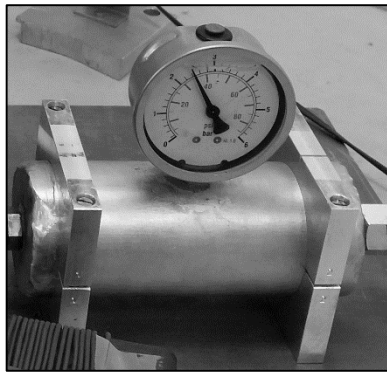

- Amyotte, P. (2013). *An introduction to dust explosions understanding the myths and realities of dust explosions for a safer workplace*. USA: Elsevier Inc.
- Attenborough, M. (2003). *Mathematics for Electrical and Computing*. Burlington, MA: Elsevier Science.
- Bartknecht, W. (1993). *Explosionsschutz - Grundlagen und Anwendung*. Springer-Verlag (ISBN-3-540-55464-5).
- BIA. (1997). *BIA-report 13/97: Combustion and explosion characteristics of dusts*. Sankt Augustin: HVBG - Federation of Statutory Accident Insurance Institutions of the Industrial Sector. ISBN3-88383-469-6.
- Bourne, M. (2016, November 15). *Interactive Mathematics*. Retrieved from Interactive Mathematics Web site: <http://www.intmath.com>
- Boyle, A. R., & Llewellyn, F. J. (1950). The electrostatic ignitability of dust clouds and powders. *Journal of the Society of the Chemical industry. Transactions*, 69, 173-181.
- Chapek, R. M., & Neville, D. L. (n.d.). *National Center for microgravity Research*. Retrieved November 03, 2016, from <https://ntrs.nasa.gov/archive/nasa/casi.ntrs.nasa.gov/20050195845.pdf>
- Eckhoff, R. K. (1970). *The energy required for the initiation of explosions in dust clouds by electric spark*. UK: M. Phil. thesis, University of London.
- Eckhoff, R. K. (1975). Towards absolute minimum ignition energies of dust clouds. *Combustion and flame*, 24, 53-64.
- Eckhoff, R. K. (2003). *Dust explosion in the process industries*. USA: Elsevier Science.
- Eckhoff, R. K. (2005a). *Explosion hazards in the process industries*. Houston, TX: Gulf professional publishing (an imprint of Elsevier).
- Eckhoff, R. K. (2016). Ignition of dust clouds by strong capacitive electric sparks of short discharge time. *11th ISHPMIE (Internation Symposium on Hazards, Prevention and Mitigation of Industrial Explosions)*. Dalian, China.
- Eckhoff, R. K., & Enstad, G. G. (1976). Why are "long" electric sparks more effective dust explosion initiators than "short" ones? *Combustion and Flame*, 27, 129-131.
- Eckhoff, R. K., & Randeberg, E. (2005b). A plausible mechanism for initiation of dust explosions by electrostatic spark discharges. *Verein Deutscher, VDI-Berichte No. 1873* (Dusseldorf, Germany), 185-197.
- Enstad, G. G. (1981). *Effect of shock waves emitted from electric spark discharges on the energies required for spark ignition of dust clouds*. Bergen, Norway: Chr. Michelsen Institute (presently CMR/ Gexcon).
- Faber, M. (1985). Sensoren in der Sicherheitstechnik von Explosionsgeschützten Industrieanlagen. *Technisches Messen tm*, 273-276.
- Glor, M. (1988). *Electrostatic Hazards in Powder Handling*. Research Studies Press Ltd., John Wiley & Sons Inc.

- Hodgman, C. D., & Lange, N. A. (1925). *Handbook of chemistry and physics*. Cleveland, OH: Chemical rubber publishing Co.
- Hong, A. (2000). *The Physics factbook*. Retrieved from Hypertextbook Web site: <http://hypertextbook.com/facts/2000/AliceHong.shtml>
- Kauffman, C. W. (1982). *Agricultural dust explosions in grain handling facilities. Proceedings of the conference. "Fuel air explosions*. Montreal, CA: University of Waterloo Press.
- Kumar, N. C. (2008). *The textbook of botany*. New Delhi: Himalaya publishing house.
- Laar, G. F., & Zeeuwen, J. P. (1985). On the minimum ignition energy of dust/air mixtures. *Archivum Combustionis*, 5, 145-159.
- Li, G., Yang, C., Ge, S., & Eckhoff, R. K. (2016). A catastrophic aluminum alloy dust explosion in China in 2014. *Journal of Loss Prevention in the Process Industries*, 19, 121-130.
- Line, L. A., Rhodes, H. A., & Gilmer, T. E. (1959). The spark ignition of dust clouds. *Journal of Physical Chemistry*, 63, 290-294.
- Margaret, E. (2008). *Practical Manual for Botany Vo. I*. New Delhi: New Age International (p) Ltd., Publishers.
- Matt, S. R. (2013). *Electricity and Basic Electronics*. USA: The Goodheart-Willcox Company, Inc.
- Moore, P. W., Sumner, J. F., & Wyatt, R. M. (1956). *ERDE Report*.
- Morgan, L., & Supine, T. (2008). Five ways new explosion venting requirements for dust collectors affect you. *Powder and Bulk Engineering*, 42-49.
- NFPA. (2007). *NFPA 68, Standard on explosion protection by deflagration venting*. Quincy, MA: National Fire Protection Association.
- Occupational Safety and Health Administration. (1992). *Process Safety Management of Highly Hazardous Chemicals, 29 CFR 1910.119*. Washington, D.C.: Occupational Safety and Health Administration.
- Olsen, W., Arntzen, B. J., & Eckhoff, R. K. (2015). Electrostatic dust explosion hazard - towards a < 1 mJ synchronized-spark generator of determination of MIEs of ignition sensitive transient dust clouds. *Journal of Electrostatics*, 74, 66-72.
- Priede, T. (1958). *Initiation of explosions in gases*. UK: PhD thesis, University of London.
- Randeberg, E., & Eckhoff, R. K. (2004). Initiation of dust explosions by electric spark discharges triggered by the explosive dust itself. *International symposium on hazards, prevention, and mitigation of industrial explosions*. Krakow.
- Randeberg, E., Olsen, W., & Eckhoff, R. K. (2006b). A new method of generation of synchronised capacitive sparks of low energy. *Journal of electrostatics*, 64, 263-272.
- Rigas, F., & Amyotte, P. (2012). *Hydrogen safety*. Boca Rayon, FL: CRC Press, Tayloy & Francis Group.

- Salam, M. A., Anis , H., Morshedy, A. E., & Radwan, R. (2000). *High - Voltage Engineering Theory and Practice*. New York: Marcel Dekker Inc.
- Scholl, E. W. (1989). Vorbeugender Explosionsschutz durch Vermeiden von wirksamen Zundquellen. *VDI-Verlag GmbH, 701, 477-489*.
- Sigma - Aldrich. (2014). Safety data sheet product no. 19108. USA: Sigma - Aldrich.
- Smith, P. W. (2002). *Transient Electronics: Pulsed Circuit Technology*. West Sussex, ENG: John Wiley & Sons Ltd.
- Thomas, G. O., Oakley, G., & Brenton, J. (1991). Influence of the morphology of lycopodium dust on its minimum ignition energy. *Combustion and Flame, 85(3-4), 526-528*.
- Wadha, C. L. (2007). *High voltage engineering*. New Delhi: New age international limited.
- Wikipedia.org. (2016, 09 23). *Wikipedia*. Retrieved 11 05, 2016, from [https://en.wikipedia.org/wiki/Cool\\_flame](https://en.wikipedia.org/wiki/Cool_flame)

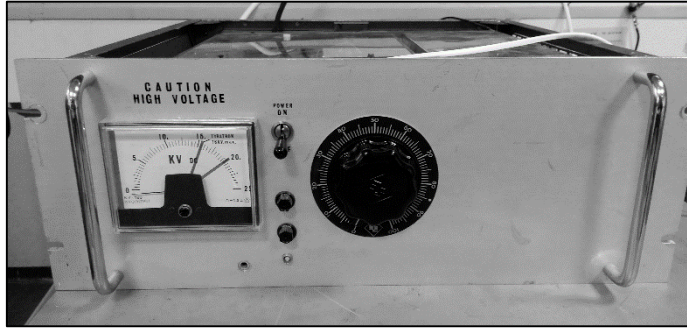


## Appendix A Experimental apparatus and measuring instruments

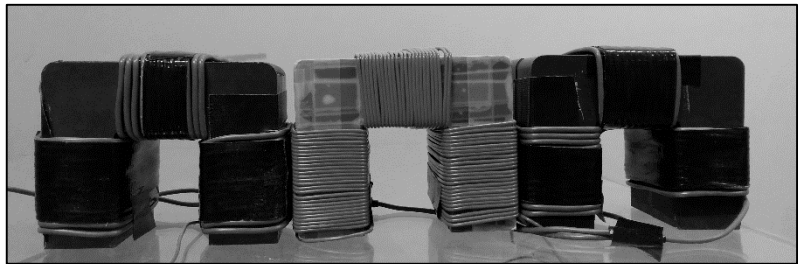
Instruments	
Capacitors	
Converter	
Cylindrical air reservoir	
Function generator	

## Instruments

High-voltage supply



Inductors



Photron high speed camera



Portable LCR meter



Resistors



**Instruments**

Solenoid valve



Steel plate for measuring spark gap



Tektronix P6015A high-voltage probe



Tektronix TDS 2002 oscilloscope



**Instruments**

Trek 542  
Electrostatic  
voltmeter with sensor  
element



Weighing scale



## Appendix B Flamelet

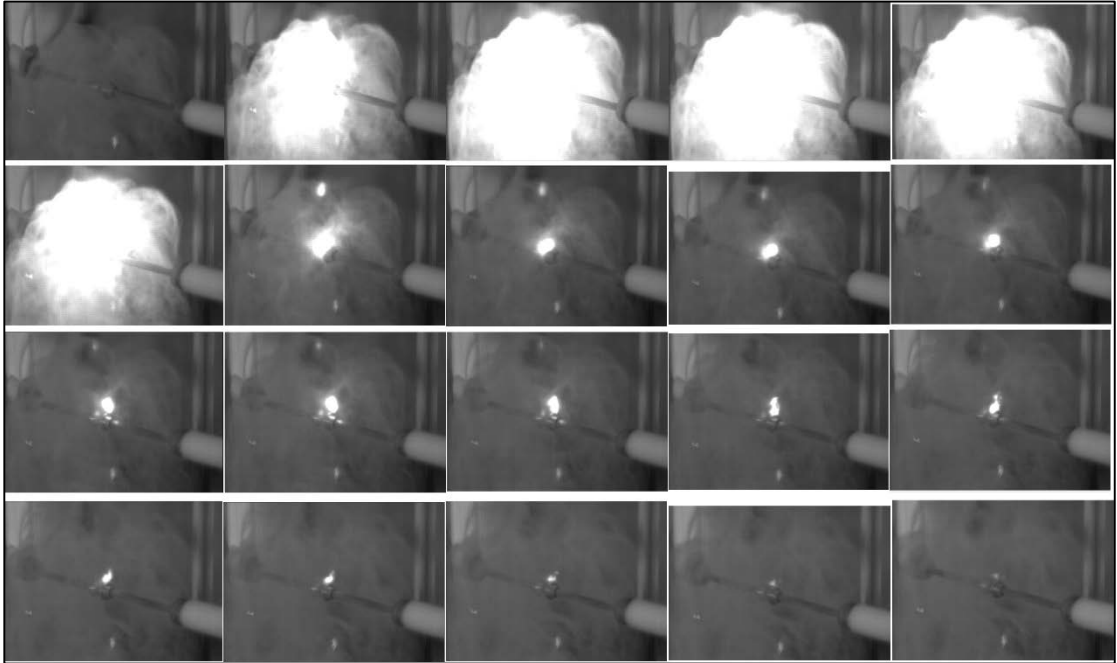


**Figure B-1: Flamelet**